Scientific Excellence • Resource Protection & Conservation • Benefits for Canadians
Excellence scientifique • Protection et conservation des ressources • Bénéfices aux Canadiens

Wind Tunnel Experiments to Determine Correction Functions for Shipboard Anemometers

M.L. Thiebaux

Published by:

Physical and Chemical Sciences
Scotia-Fundy Region
Department of Fisheries and Oceans

Bedford Institute of Oceanography
P.O. Box 1006
Dartmouth, Nova Scotia
Canada B2Y 4A2

March 1990

Canadian Contractor Report of Hydrography and Ocean Sciences No. 36

Fisheries and Oceans Pêches et Océans

Canada

Canadian Contractor Report of Hydrography and Ocean Sciences

Contractor reports are unedited final reports from scientific and technical projects contracted by the Ocean Science and Surveys (OSS) sector of the Department of Fisheries and Oceans.

The contents of the reports are the responsibility of the contractor and do not necessarily reflect the official policies of the Department of Fisheries and Oceans.

If warranted, contractor reports may be rewritten for other publications of the Department, or for publication outside the government.

Contractor reports are abstracted in *Aquatic Sciences and Fisheries Abstracts* and indexed in the Department's annual index to scientific and technical publications.

Contractor reports are produced regionally but are numbered nationally. Requests for individual reports will be filled by the issuing establishment listed on the front cover and title page. Out of stock reports will be supplied for a fee by commercial agents.

Regional and headquarters establishments of Ocean Science and Surveys ceased publication of their various report series as of December 1981. A complete listing of these publications is published in the *Canadian Journal of Fisheries and Aquatic Sciences*, Volume 39: Index to Publications 1982. The current series, which begins with report number 1, was initiated in January 1982.

Rapport canadien des entrepreneurs sur l'hydrographie et les sciences océaniques

Cette série se compose des rapports finals non révisés préparés dans le cadre des projets scientifiques et techniques réalisés par des entrepreneurs travaillant pour le service des Sciences et levés océaniques (SLO) du ministère des Pêches et des Océans.

Le contenu des rapports traduit les opinions de l'entrepreneur et ne reflète pas nécessairement la politique officielle du ministère des Pêches et des Océans.

Le cas échéant, certains rapports peuvent être rédigés à nouveau de façon à être publiés dans une autre série du Ministère, ou à l'extérieur du gouvernement.

Les rapports des entrepreneurs sont résumés dans la publication *Résumés des sciences halieutiques et aquatiques* et ils sont classés dans l'index annuel des publications scientifiques et techniques du Ministère.

Les rapports des entrepreneurs sont produits à l'échelon régional, mais numérotés à l'échelon national. Les demandes de rapports seront satisfaites par l'établissement auteur dont le nom figure sur la couverture et la page du titre. Les rapports épuisés seront fournis contre rétribution par des agents commerciaux.

Les établissements des Sciences et levés océaniques dans les régions et à l'administration centrale ont cessé de publier leurs diverses séries de rapports en décembre 1981. Une liste complète de ces publications figure dans le volume 39, Index des publications 1982 du *Journal canadien des sciences halieutiques et aquatiques*. La série actuelle a commencé avec la publication du rapport numéro 1 en janvier 1982.

Canadian Contractor Report of
Hydrography and Ocean Sciences No. 36

March 1990

WIND TUNNEL EXPERIMENTS TO DETERMINE CORRECTION FUNCTIONS FOR SHIPBOARD ANEMOMETERS

M.L. Thiebaux

Seakem Oceanography Limited
P.O. Box 696
Dartmouth, Nova Scotia B2Y 4A2
Telephone: (902) 463-0932 FAX: (902) 464-9602

Published by:

Physical and Chemical Sciences
Scotia-Fundy Region
Department of Fisheries and Oceans

Bedford Institute of Oceanography
Dartmouth, Nova Scotia
Canada B2Y 4A2

90-04320/

© Minister of Supply and Services 1990
Cat. No. Fs 97-17/36E ISSN 0711-6748

Correct citation for this publication:

Thiebaux, M.L., Seakem Oceanography Limited. 1990. Wind Tunnel Experiments to Determine Correction Functions for Shipboard Anemometers. Can. Contractor Rep. Hydrogr. Ocean Sci. No. 36: iv + 57 pp.

ABSTRACT

Thiebaux, M.L., Seakem Oceanography Limited. 1990. Wind Tunnel Experiments to Determine Correction Functions for Shipboard Anemometers. Can. Contractor Rep. Hydrogr. Ocean Sci. No. 36: iv + 57 pp.

A boundary-layer wind-tunnel experiment is described in which correction functions for shipboard anemometers were determined. Scale models of the C.S.S. Dawson, C.S.S. Baffin, and C.S.S. Hudson, each carrying the regular ship anemometer and an experimental bow anemometer, were tested. Angular error and speed correction functions are plotted and tabulated in this report and their application to the measurement of unknown wind fields is demonstrated. The functions are specific to nonmoving ships in neutrally stable wind fields with 10 meter height drag coefficients ranging upwards of 1.59×10^{3}. More extensive testing was carried out on the Dawson, including higher wind speeds, pitched and rolled ship orientations, and different bow anemometer heights. The results are discussed to point out and explain features that are consistent or contrasting among the ships.

RESUME

Thiebaux, M.L., Seakem Oceanography Limited. 1990. Wind Tunnel Experiments to Determine Correction Functions for Shipboard Anemometers. Can. Contractor Rep. Hydrogr. Ocean Sci. No. 36: iv + 57 pp.

Une expérience en soufflerie sur la couche limite, qui a permis de déterminer des fonctions de correction pour les anémomètres à bord de navires, est décrite. Des modèles à l'échelle des navires hydrographiques canadiens Dawson, Baffin et Hudson portant chacun l'anémomètre de bord ordinaire et un anémomètre d'étrave expérimental ont été mis à l'épreuve. Les fonction de correction pour l'erreur angulaire et la vitesse sont portées sur graphique et présentées sous forme de tableaux dans ce rapport qui comporte également une démonstration de leur application à la mesure de champs de vent inconnus. Les fonctions sont spécifiques à des navires à l'arrêt dans des champs de vent de stabilité neutre et présentant des confficients de traînée à une hauteur de 10 mètres échelonnés et supérieurs à $1,59 \times 10^{3}$. Des essais plus élaborés ont été effectués à bord du Dawson, dont des essais avec des vitesses du vent plus élevées, des essais lorsque le navire était soumis au roulis et au tangage et des essais avec l'anémomètre d'étrave placé a différentes hauteurs. Les résultats sont discutés afin de souligner et d'expliquer les éléments uniformes ou contrastés d'un navier à l'autre.

TABLE OF CONTENTS

1. INTRODUCTION 1
1.1 Background 1
1.2 Error Types and Their Correction 1
1.3 Review of Previous Work 3
1.4 Present Approach 6

2. WIND TUNNEL EXPERIMENTS -- FACILITIES AND APPARATUS 7
2.1 Boundary Layer Wind Tunnel Laboratory 7
2.2 Ship Models. 8
2.3 Experimental Setup 8

3. WIND TUNNEL EXPERIMENTS -- MEASUREMENTS 10
3.1 Overview of Experiments 10
3.2 Self-Similarity 12
3.3 Vertical Wind Profiles 13
3.4 Angle Measurements 17
3.5 Application of Angular Errors 19
3.6 Speed Measurements 21
3.7 Application of Speed Correction Functions 23
3.8 Wind Tunnel Blockage 23

4. WIND TUNNEL RESULTS 24
4.1 Displayed Correction Functions 24
4.2 Symmetries 25
4.3 Regular Anemometer Experiments 26
4.3.1 Angular Errors 26
4.3.2 Speed Correction Functions 26
4.3.3 Discussion 27
4.4 Additional Dawson Experiments 28
4.4.1 Vertical Wind Profile Experiments 28
4.4.2 Pitch Experiments 28
4.4.3 Roll Experiments 29
4.4.4 Bow Anemometer Height Experiments 30

5. SUMMARY, CONCLUSIONS AND DISCUSSION 30

6. ACKNOWLEDGEMENTS 32

7. REFERENCES 33

TABLES
1. Vertical wind profile parameters 16
2. Partial test sequence results for Dawson (angle measurements) 19
3. Partial lookup table for Dawson angular errors 20
4. Partial test sequence results for Dawson (speed measurements) 22
5. Anemometer Corrections for C.S.S. Dawson 35
6. Anemometer Corrections for C.S.S. Baffin 36
7. Anemometer Corrections for C.S.S. Hudson 37

FIGURES 38-57

1. INTRODUCTION

1.1 Background

Shipboard anemometer wind measurements are subject to serious inaccuracies, although the measurements are an important direct source of marine wind information. Wind speed and direction errors affect daily onboard operations, such as navigation and routine meteorological observations. The errors have more serious implications for measurements made for research and operations in local and synoptic-scale marine meteorology. Such applications are dependent on the space-time differential properties of the wind field that may easily be masked by the size of the measuring errors (Romanov et al, 1983). The reduction of potential errors to about 2 percent in speed and 3 degrees in direction is desirable for these applications (Romanov et al, 1983; Wucknitz, 1980; Blanc, 1986).

1.2 Error Types And Their Correction

Aside from inherent instrumentation errors, four types of error can be identified. The first two are relatively easy to correct or estimate, being kinematical in nature; the other two have dynamical sources, involving the aerodynamics of the anemometer and the aerodynamics of the ship, and are difficult to treat. Types (1), (2), and (3) are defined in the idealized situation where the presence of the ship is nonintrusive, i.e. the ship does not disturb the wind field, while type (4) directly addresses the intrusive presence of the ship:

(1) Let the average apparent wind vector at an anemometer site be called the anemometer wind. On a nonintrusive moving ship platform (coordinate system moving at ship speed), the relative wind profile and in particular the anemometer wind differ from the true or earth referenced wind. The gross part of this error is corrected by simply adding the average velocity vector of the ship to the average anemometer wind to obtain a better approximation to the earth referenced wind vector at anemometer height. For a ship in uniform linear motion in a steady wind field this procedure would completely correct the error. It should be noted that the relative wind profile under these circumstances has a generally

spiral structure (the relative wind direction and speed change with height) unless the wind and ship directions are parallel or antiparallel.

(2) In practice the ship platform is not in uniform motion. The anemometer samples the wind field in a path which oscillates about a mean uniform motion. A bias is induced in the anemometer wind due to the nonlinear vertical variation of the wind field. If the moving platform is assumed to be nonintrusive, this error could in principle be corrected completely if more detailed information on the motion of the ship and on the spatial structure of the wind field (or at least its analytical form) were available. However the error should normally be very small. For example in the severe case of an anemometer undergoing vertical 5 m amplitude simple harmonic motion about a mean height of 20 m and sampling a 25 m/s wind, the average wind speed would be underestimated by less than 0.2 percent.

(3) Additionally there is a complex group of errors related to the aerodynamical properties of a mechanical wind sensor the supports of which are subject to linear accelerations and angular displacements when the ship platform is not in uniform motion. Included in this group of errors is the possibly inaccurate response of the sensor when the wind field itself is not steady. These errors, due to vibration, non-cosine response, cup overspeeding, etc., also should normally be small. Again if the moving platform is assumed to be nonintrusive, these errors could be corrected in principle if in addition to more detailed information on the ship's motion and the structure of the wind field, the appropriate mechanical and aerodynamical properties of the anemometer were known.

(4) The notion of a nonintrusive ship is an idealization and a fiction. The hull and superstructure of the ship appreciably distort the air flow in the neighborhood of the ship. The ship

anemometer, generally located amidships just above the obstruction presented to the wind, samples this distorted field and yields an anemometer wind with appreciable errors. While the first three types of errors are independently treatable on an idealized nonintrusive platform, the type (4) (or blockage) error is neither obviously separable nor easily corrected.

The presence of type (4) blockage error confounds types (1) and (2) kinematic errors so that they cannot rigorously be treated separately from the ship blockage error. For example, type (1) error is trivially correctable in the absence of ship blockage because the relative wind linearly separates into true wind minus ship motion vector. The anemometer wind in the presence of ship blockage depends nonlinearly on the distribution of the relative wind profile over the ship hull and superstructure. Hence simply subtracting the ship velocity from the anemometer wind is not rigorously correct in the presence of ship blockage. Nevertheless, considering that ship blockage is traditionally ignored, while type (1) error is traditionally corrected, it seems better to go ahead with the type (1) correction as though it were a separable correction for any ship and any wind regime.

The simplest case of type (4) error would be that of a nonmoving ship in a stationary wind field in which case the relative wind profile is identical to the true wind profile, the wind is unidirectional, and types (1) to (3) errors are zero.

1.3 Review of Previous Work

Using published estimates of weather-ship sensor accuracies and ship-induced distortions, Blanc (1986a) looked at the corresponding uncertainties of bulk-derived atmospheric fluxes of momentum, heat, and humidity. These fluxes lie at the heart of the atmosphere-ocean interaction, determining weather, climate, and sea state. Bulk methods rely on a variety of schemes that relate routine surface meteorological observations to atmospheric fluxes. Wind speed is always needed since turbulent mixing is the principal mechanism driving the exchanges. Blanc determined that the major sources of

uncertainty in the bulk-derived parameters were wind speed, temperature, and humidity measurements. Some typical derived uncertainties found were 30% for wind stress and 50% for the heat fluxes. The employment of ship models in a boundary-layer wind tunnel to get accurate speed measurements was suggested. Blanc concluded that "For a given mast location and type of ship, it is hoped that a correction algorithm can be developed which can be used to compute the true wind speed and direction as if the ship were not present."

In a later paper Blanc (1986b) derived such algorithms for the USN Tarawa, a 250 m helicopter assault ship. Experiments similar to those described in this project were conducted on a scale model of the ship in the atmospheric boundary-layer simulation wind tunnel operated by British Maritime Technology, Teddington, England. The algorithms are presented in the form of interpolated tables giving wind speed correction factors and angular corrections for 5-degree increments of observed wind directions for both the port and starboard anemometers. The corrections apply to a level nonmoving ship and are assumed to be most applicable to the neutral stability case and a mid-range value of roughness length. (These terms are defined in the footnote on page 14). Blanc gave estimates of the variation of wind speed corrections due to typical deviations from neutrality and mid-range roughness. Blanc pointed out that angle-dependent corrections must be specifically tailored to ship type and anemometer location.

Romanov et al (1983) reported wind tunnel experiments of a 1:100 scale model of the R/V Akademik Mstislav Keldysh (6340 tons displacement). The tests were carried out for a level ship exposed to a 180 degree range of wind directions in the wind tunnel (not described as a boundary-layer wind tunnel). Vertical and horizontal deflection angles as well as the relative distortion in wind speed were measured at 3 principal locations: bow boom, foremast, and mainmast. These investigators recognized that although the determination of the most favorable sites for shipboard anemometers is desirable, no site would be completely free of distortions, and hence the important pursuit is to measure quantitatively the distortion of the wind at the anemometer locations. They also pointed out that ships of different architectures should be studied in wind tunnels, that it would

be useful to determine corrections for all USSR research vessels, and that the corrections could be entered in handbook tables as is done for other ship data.

A study of wind measurements on a 1:300 scale model jackup rig conducted at the Boundary Layer Wind Tunnel Laboratory at the University of Western Ontario (Vickery et al, 1985) looked at mean speeds, turbulence levels, gust factors, and spectra in a boundary-layer flow corresponding to strong winds over water. Wind deflection angles were not investigated. Field tests on a full scale jackup rig had been carried out at a site just east of Sable Island in 1980-1981. The purpose of the wind tunnel tests was to determine the influence of the rig on the field data. Wind tunnel measurements were made with the model present and compared to the corresponding measurements at the same position but with the model removed. The location of the anemometer was such that winds from some directions were severely distorted by the rig structure (legs). Directions of markedly increased turbulent intensity were also characterized by increased gust factor, reduced mean speed, and distorted spectra. There was a small range of directions where the rig caused negligible distortion of the spectra. These were also regions of increased speed but negligible errors in turbulence and gust factors. The applicability of correction factors for the wind spectra was suspect since the distortion of the turbulent intensity was generally so great.

A large correction factor for some component of the wind, whether spectral or mean, is considered unreliable if there is poor correspondence between the full scale and model components in the free stream. With adequate free stream modeling of the mean speed alone (probably the typical case in wind tunnel modeling) there is then the implication that shipboard anemometer correction factors can be confidently determined for mean wind velocity components but perhaps not for turbulent intensities or spectra. There is a some conceptual difficulty with this argument, however, in that the mean profile is determined at least in part by the turbulent intensity profile through the momentum transfer balance.

1.4 Present Approach

This project treats the special case of the ship blockage error (type 4) for a nonmoving ship. Tests with scale models of ships in a boundary layer wind tunnel were undertaken to provide a reproducible laboratory environment in which the errors can be measured with precision. The Bedford Institute of Oceanography (BIO) showcase models of the C.S.S. Dawson, C.S.S. Baffin, and C.S.S. Hudson were used in the wind tunnel tests. These finely detailed models were kindly loaned to the project by the BIO Ships Division.

Nonmoving blockage errors for the C.S.S. Dawson were also measured in a series of field experiments conducted in June - November 1988 (Anderson, 1990). The Dawson was equipped with a specially installed bow anemometer (Gill propeller-vane) as well as the regular U2A shipboard anemometer. Simultaneous measurements of the ambient wind were taken from an R.M. Young anemometer on a Coastal Climate "Minimet" buoy moored at a distance of about 1 km.

The objective of the wind tunnel and field experiments is to determine correction functions to apply to the anemometer wind to obtain the true wind at anemometer height. Specifically, lookup tables are developed that associate an additive angular error and a multiplicative speed ratio error with any observed anemometer wind direction. Strictly speaking, the tables would be limited to nonmoving blockage errors for the specific ships tested, and possibly to narrow ranges of wind speeds. With some caution the results can also be applied to moving ships where the gross part of type (1) error is corrected, and to wider ranges of wind speeds.

2. WIND TUNNEL EXPERIMENTS -- FACILITIES AND APPARATUS

2.1 Boundary Layer Wind Tunnel Laboratory

The anemometer heights on the three ships studied in this report range from 19 to 26 meters. In the lower few hundred meters of the earth's atmosphere (planetary boundary layer) the wind speed increases logarithmically with height. Over the vertical extent of the hull and superstructure of the Hudson for example, from a height of one meter to 26 meters, the increase of wind speed can be over 40%. Hence it is necessary to conduct the tests in a wind tunnel which simulates the logarithmic wind profile of the planetary boundary layer. Boundary layer wind tunnels are commonly used to study wind loads on large stationary structures such as buildings and bridges. The vertical wind profile and degree of turbulence can be controlled by adjusting roughness elements on the floor of the wind tunnel.

The experiments in this study were undertaken at the Boundary Layer Wind Tunnel Laboratory (BLWTL) at the University of Western Ontario and are described by Surry, Edey, and Murley (1989). Their report is referred to as SEM. BLWTL has 25 years of experience in studies of tall buildings, long span bridges, towers, roof systems, atmospheric diffusion, wind and wave interactions, and a great variety of other problems. The tests were conducted with the ship models mounted on a turntable in the high-speed 3.4 m wide by 2.5 m high test section of BLWT II, the larger and more technologically advanced of BLWTL's two wind tunnels. Computer-controlled roughness elements are located on the wind tunnel floor 20 meters upstream of the turntable. Progression through test sequences, wind tunnel operation, and data collection are controlled by a PDP-11/23 computer. Data analysis is carried out on a VAX 780 computer.

2.2 Ship Models

The scale of the Dawson model is 1:48 while that of the Baffin and Hudson is 1:96. The models were accurate when made, but the Baffin and Hudson have since undergone midlife refits which made substantial parts of the model superstructures obsolete. Guided by blueprints, members of the University of Western Ontario Machine Shops constructed modified sections and fitted them to the models. Some small objects such as radar antennas in the proximity of the regular anemometers differ between model and actual ship, but fidelity of the hulls and major deck structures was assured.

The heights of the regular ship anemometers are: Dawson 18.8m; Baffin 23.4m; and Hudson 25.6m above waterline. All anemometers are on the port side of the center-line by the following amounts: Dawson 1.8m; Baffin 1.6m; and Hudson 1.6m.

Only the normally above-water parts of the ships were exposed in the wind tunnel. In the case of the Dawson, the largest model, this required the construction of a false floor extending upstream and tapering onto the main floor of the wind tunnel. The Dawson, which was subjected to a more extensive series of tests than the other models, required mounting in a special rig to hold the model at fixed angles of pitch and roll. The other two models were mounted directly into the turntable.

2.3 Experimental Setup

Miniature wind probes at the anemometer sites were fixed relative to the ship by projecting them downward from supports above the ship rather than mounting them directly to the ship. The probe supports were then tied rigidly to the turntable by vertical posts fitted with self-aligning fairings to reduce to a minimum their interference with the air flow. Thus, turntable, ship, supporting system, and wind probes could rotate together as a rigid ensemble.

The wind speeds and directions at the anemometer sites were measured with miniature cylindrical probes especially developed by BLWTL for this project (Surry, McDougall, and Murley, 1989; Surry, McDougall, Murley, and Edey, 1989). Cylinders, 3.8 mm in diameter and 12 mm long, have an array of 12 pressure tap holes 0.25 mm in diameter around the central circumference. The axis of symmetry of the pressure distribution gives the wind direction. Of several methods investigated to determine the mean wind speed, the best was that of relating it to the difference between frontal stagnation pressure and the mean wake pressure. Rms errors of less than 0.5 degrees in direction and 1.5 % in speed with negligible bias were found in tests of the probes. For winds inclined to the plane of tap holes, the direction accuracy is maintained, while only the wind speed component in the plane of tap holes is sensed. Accuracy deteriorates for inclinations greater than 15 degrees; this performance is similar to cup anemometers.

A key fixture in the experimental setup is a pitot-static tube located at a fixed reference point in the free stream flow above the simulated boundary layer 1.5 meters above the wind tunnel floor and 1.7 meters upstream of the turntable center. This sensor was used to monitor the free stream speed V_g and thus provide an absolute reference wind speed during all tests. The role of a reference point will be explained below. V_g was maintained at about 15 m/s for all test sequences.

3. WIND TUNNEL EXPERIMENTS — MEASUREMENTS

3.1 Overview of Experiments

To achieve the objective of determining correction functions, two sets of measurements are required. One is that of the wind undisturbed by the ship and minimally perturbed by experimental apparatus. Effects of the wind tunnel apparatus are referred to as perturbations. The other is that of the same ambient wind field locally disturbed by ship blockage. A comparison of the sets of data by some means of analysis then yields the correction functions for the scale models, while a scaling principle is called on to apply the corrections to the real ships. Two key experimental difficulties are (1) minimizing or treating unwanted perturbations so that they have negligible effect on final results, and (2) ensuring that the ambient wind fields are the same or treating them so that they are effectively the same.

Except for the vertical profile measurements described below, all tests fall into one of two categories: NO SHIP test sequences yielding cylindrical probe measurements of the undisturbed ambient wind field at the location to be occupied by the anemometer; and, corresponding to each NO SHIP test sequence, one or more WITH SHIP test sequences giving cylindrical probe measurements of the anemometer wind with the ship present. In the NO SHIP tests the wind field is actually perturbed slightly by the presence of wind probes, supporting devices, and the walls of the wind tunnel itself, and so simulates a perturbed approximation to a true undisturbed natural wind field. The WITH SHIP tests are the same measurements now conducted with the ship present and with exactly the same perturbing influences as in corresponding NO SHIP tests. Although no ship is present in a NO SHIP test, a ship must be specified since the anemomoter locations and perturbing influences are ship-specific. The method of data analysis provides a formal mechanism for assuming the effects of the perturbing influences are the same between corresponding tests and thereby removing them.

A basic set of NO SHIP and WITH SHIP test sequences was carried out in which each ship

- was level,
- was exposed to a relatively smooth wind profile considered to be typical for marine conditions,
- bore two fixed anemometer sites: regular and bow where the bow anemometer was 1 m behind the bow, 6.5 m above deck for the Dawson, 8.5 m above deck for the Baffin and Hudson, and
- was exposed to a sequence of wind directions in 10 degree steps for the full-azimuth range.

Additional test sequences were carried out on the Dawson:

- the basic NO SHIP and WITH SHIP tests as above but for two other wind profiles (rougher and roughest);
- the basic tests but with the ship rolled 20 degrees to port and 20 degrees to starboard (WITH SHIP only);
- the basic tests but with the ship pitched bow up 5 degrees, bow down 5 degrees, each for half-azimuth range only (WITH SHIP only);
- the basic tests but with the bow anemometer 8.5 m above deck, 5.5 m above deck, each for half-azimuth range only (WITH SHIP only).

The Dawson bow anemometer was initially set at 6.5 m above the deck, or 12.5 m above waterline to agree with the Gill anemometer placement on the field tests. Subsequent tests were done at 2 m above and 1 m below the initial height. The higher height seemed to give the best result and so was used for the later Hudson and Baffin tests. A test in the full-azimuth range consisted of a sequence of 36 directions at 10 degree intervals. The half-azimuth range consisted of 19 directions at 10 degree intervals ranging from 0 to 180 degrees. Angles are measured clockwise from the bow at 0 degrees.

Counting regular and bow anemometer WITH SHIP test sequences separately, there were 10 full-azimuth and 6 half-azimuth tests on the Dawson, and 2 full-azimuth tests on each of the other models. There were 6 NO SHIP (full-azimuth) tests on the Dawson and 2 on each of the other models.

3.2 Self-Similarity

Experiments conducted in boundary layer wind tunnels depend on a self-similarity scaling principle both for the experimental procedures and analyses as well as the application of results to the real-scale world. One statement of the principle is that the ratio of any two average velocity components at two fixed locations in the wind tunnel is independent of the free stream speed (or fan power), for a given configuration of obstructions such as probe supports and the presence and orientation of a model. Practical assumptions for the operation of boundary layer wind tunnels are that (1) there is a very broad range of Reynolds numbers for which self-similarity holds, (2) experiments are conducted in this range, and (3) the real-scale wind regimes for which the experiments apply also lie in this range. In fact, self-similarity sets in for Reynolds numbers (Re) greater than some critical value which for poorly streamlined bodies corresponds to a speed of about 7 m/s for a 1 meter long model or about 7 cm/s for a 100 m ship (Romanov et al., 1983). These quoted speeds apply to self-similarity for the entire hull, The Re may be too low to attain true self-similarity for small details, such as masts, in this study.

Note that self-similarity implies that the wind direction field is independent of the free stream speed. Also absolute measurements of wind speed are not especially significant even in cases where the free stream speed or fan power could be controlled precisely, whereas speed ratios are meaningful quantities and independent of fan power. Note also that if the speed measurements could be taken with the same instrument, then any systematic multiplicative error exactly cancels in the ratio.

Again with the exception of the vertical wind profile measurements, the present application is a little more complicated since it involves two different instruments used for simultaneous speed measurements at different

locations for one configuration of obstructions (WITH SHIP) within the wind tunnel, and then a repeat set of measurements for a different configuration of obstructions (NO SHIP). Let P' and Q' be average speed measurements respectively near and far from an object in the wind tunnel. Now remove the object and let P and Q be the speed measurements at exactly the same locations. If we could finely tune the wind tunnel power so that the far (ambient) speeds are equal (Q' = Q), then the effect of the object on the near wind speed would be the ratio P'/P. With self-similarity there is no need for fine tuning; the multiplicative effect of the object on the near speed is given by (P'/P)/(Q'/Q) = (P'/Q')/(P/Q), i.e. the ratio of speed ratios. Note that we have the added plus that any systematic multiplicative errors for the two instruments exactly cancel out of this form. In our application Q' and Q represent the reference point speed measurements V_g taken with the pitot-static tube.

3.3 Vertical Wind Profiles

Vertical wind profile measurements were carried out at the ship location with no ship present by traversing the wind tunnel from floor to ceiling with a hot-film anemometer while monitoring the reference point wind speed. As in all speed measurements in this study, the vertical wind profile data is formulated in terms of a "normalized" wind speed, the ratio u of the hot-film anemometer speed to the reference point speed V_g. An example of a vertical wind profile for the Dawson experimental setup is presented in Figure 1.

Four different vertical profiles were set up and measured: three for the Dawson, called smooth, rougher, and roughest; and one for the Baffin and Hudson which on the real scale of the wind tunnel was very nearly the same as the Dawson smooth. There was some difference between the Baffin/Hudson profile and the Dawson smooth probably due to the raised floor for the Dawson. SEM fit the experimental data to a power law form $u = (z/z_g)^{\alpha}$ where z is the scale height above sea level.

Here we refit the data to the familiar logarithmic form of the wind profile in a frictional, neutrally stable boundary layer,

$$U(Z) = (u*/k)\ \ln(\ Z/z_0\ ), \tag{1}$$

where $U(Z)$ is the speed at height Z, $u*$ is called the friction velocity, z_0 is defined as the roughness length of the underlying surface, and $k = 0.4$ is the von Karman constant.[1] The roughness of the sea surface is determined by the waves which in turn are dependent on the wind. By combining formulas of Charnock (1955) for z_0 at higher wind speeds with a viscous flow formula for lower wind speeds, Smith (1981, 1988) tabulated the 10 meter height drag coefficient $C_{10} = (u*/U_{10})^2$ for the sea surface as a function of $U_{10} = U(10\ m)$ for wind speeds up to 25 m/s. Note that from Equation (1) and the definition of C_{10}, the roughness length is directly related to the drag coefficient by the formula $z_0 = \exp(-k/C_{10}^{1/2})\ x\ 10m$. We proceed to show that for a given U_{10}, an explicit representation of the vertical wind profile can be formed from Equation (1) using Smith's table. In the following, Z and z_0 are measured in meters. From Equation (1),

$$\begin{aligned} U(Z) - U_{10} &= (u*/k)\ [\ln(Z/z_0) - \ln(10/z_0)\ ] \\ &= (u*/k)\ (\ln Z\ -\ \ln 10), \\ U(Z) \quad &= U_{10}\ [\ 1 + (u*/kU_{10})(\ln Z - \ln 10)\ ] \\ &= U_{10}\ [\ 1 + (C_{10}^{1/2}/k)\ \ln(Z/10)\ ]. \end{aligned} \tag{2}$$

Now we introduce a normalizing factor f so that the real-scale wind speed is related to the normalized wind speed in the tunnel, $u(z)$:

$$U(Z) = fu(z). \tag{3}$$

Here z is the dimensionless scaled height, which for example takes a value

---

[1] A boundary layer is said to be neutrally stable if, when an air parcel is moved up or down adiabatically (no heat exchanged with its surroundings) and then brought to a stop, there is no tendency for further motion. The roughness length is the height at which the wind speed goes to zero in the logarithmic profile form.

of 10 at a height corresponding to 10 m on the ship model. As long as Z is measured in meters, z and Z are identical. We can fit a logarithmic profile to the wind tunnel data,

$$u(z) = A + B \ln(z/10), \tag{4}$$

by a least squares determination of A and B. From Equation (3) at a height of 10 m we see that

$$U_{10} = fA \tag{5}$$

and so from Equation (2)

$$U_{10} C_{10}^{1/2} / k = fB$$
$$C_{10} = (kB/A)^2. \tag{6}$$

Regarding the deviations of the data from the analytic fit as random fluctuations, we can estimate the variances and covariance of A and B by well-known formulas and hence the standard errors of functions of A and B. For relatively small variances (Kendall and Stuart, 1961),

$$\mathrm{var}(B/A) = (B^2/A^2)[\mathrm{var}(A)/A^2 + \mathrm{var}(B)/B^2 - 2\mathrm{cov}(A,B)/AB], \tag{7}$$

which is used to estimate the standard error of C_{10}.

Equation (6) shows that the logarithmic fit to the normalized wind tunnel profile uniquely determines the simulated drag coefficient (and roughness length). I.e., these profile parameters are independent of the normalization factor f. However, without some further relation, U_{10} as well as f and u_* cannot be determined. We can use an empirical relation giving the drag coefficient C_{10} as a function of U_{10} (e.g. Smith, 1981, 1988) by inverting the function to determine what wind speed has been simulated, since C_{10} is known explicitly from Equation (6). Smith's tabulated relation is based on an algorithm that allows analytic continuation in principle to any value of U_{10}, although continuation beyond 25 m/s is not justified experimentally. Table 1 lists the profile parameters obtained from the logarithmic fit to the wind tunnel measurements

of the four vertical wind profiles, as well as U_{10}, derived from the empirical relation. We find that except for the "Dawson smooth" profile (U_{10} = 15.7 m/s) the profiles used lead to wind speeds of 27 to 118 m/s which are beyond the range of experimental data on the drag coefficient. Determining the wind speed in this way is risky since the drag coefficient varies relatively slowly with wind speed; the size of this variation is still in debate and depends also on other parameters such as sea state and stability. A more reasonable alternative interpretation is to acknowledge that the simulated wind speeds are indeterminate and that the wind tunnel profiles correspond to a somewhat higher drag coefficient and roughness length than is typical of open-sea conditions.

Table 1. Vertical wind profile parameters

Profile	10xA	100xB	$10^3 x C_{10}$	z_0 (mm)	U_{10} (m/s)
Dawson /smooth	8.45 ±0.03	8.44 ±0.18	1.59 ±0.07	0.45 ±0.10	15.7 ±1.4
Dawson /rougher	7.68 ±0.07	9.50 ±0.49	2.45 ±0.27	3.1 ±1.4	33.5 ±5.7
Dawson /roughest	6.58 ±0.11	15.2 ±0.7	8.60 ±0.96	134 ±32	118 ±8
Baffin & /Hudson	7.69 ±0.03	8.90 ±0.2	2.15 ±0.09	1.78 ±0.32	27.2 ±1.9
Open sea	--	--	1.30	0.15	10
Open sea	--	--	1.56	0.40	15
Open sea	--	--	2.04	1.43	25

The last three lines of Table 1 contain some expected values of C_{10} and z_0 for neutrally stable, open sea conditions according to Smith's table. In comparison, the "Dawson roughest" profile corresponds to a rougher surface than the sea but could possibly represent a ship surrounded by pack ice.

3.4 Angle Measurements

A number of angles are defined in SEM. These and additional angles are defined below and illustrated in Figure 2. All angles, except error and perturbation angles, are measured clockwise from the ship axis (ship's bow).

w = undisturbed wind direction. "Undisturbed" means undisturbed by virtue of there being no ship blockage. w is perturbed slightly by wind tunnel obstructions, such as probe support posts, that are however in exactly the same positions in corresponding NO SHIP and WITH SHIP tests.

n = NO SHIP observed angle. This is called the "reference observed angle" and "true angle" in SEM.

t = turntable angle. This is also called "nominal wind angle" and "indicated angle" in SEM. Note that t is regarded as precisely repeatable, and provides common reference points between NO SHIP and WITH SHIP tests.

p = observed angular perturbation, the difference between turntable angle and NO SHIP observed angle. This is called "angular perturbation" in SEM.

a = systematic probe error = sum of probe alignment and inherent errors (small inseparable unknown constant errors)

e = perturbation error, the difference between turntable angle and undisturbed wind direction. This error is probably primarily the perturbation caused by the vertical posts supporting the cylindrical probes. In the absence of any perturbing influences, as in an empty wind tunnel, it is assumed that e = 0, so that the undisturbed direction of the wind would be identical to t.

From Figure 2a:

$$t = n + a + e$$
$$p = t - n \qquad (8)$$
$$w = n + a.$$

Figure 2b illustrates the relationships among the angles defined below for the WITH SHIP tests.

w' = disturbed wind direction, measured clockwise from the bow.

n' = WITH SHIP observed angle (called "observed angle" in SEM).

t, a are the same as in the NO SHIP case.

From Figure 2b:

$$w' = n' + a. \qquad (9)$$

The angular error E is defined as the difference between the disturbed and undisturbed wind directions, or equivalently the difference between the WITH SHIP and NO SHIP observed angles:

$$E = w' - w = n' - n. \qquad (10)$$

Note that the systematic probe error cancels out.

For each value of t in the NO SHIP and WITH SHIP test sequences, values of n and n' are measured and p and E are computed. Although at this point it is natural to regard t as the independent variable connecting p, n, n', and E, it is informative to eliminate t and regard n' as the independent variable, thus obtaining a display table of values of p and E as a function of n'. Plotted results of the wind tunnel tests for E are presented in this form in SEM. Table 2 illustrates these steps with a portion of the test sequence for the regular anemometer on the level Dawson exposed to the smooth wind profile.

Table 2. Partial test sequence results for Dawson (angle measurements)

NO SHIP			WITH SHIP		Display Table		
t	p(t)	n(t)	n'(t)	E(t)	n'	p(n')	E(n')
deg	deg	deg	deg	deg	deg	deg	deg
...	...	...	...	...	...	...	...
-20	-0.3	-19.7	-20.4	-0.7	-20.4	-0.3	-0.7
-10	-0.5	-9.5	-10.5	-1.0	-10.5	-0.5	-1.0
0	-1.0	1.0	0.8	-0.2	0.8	-1.0	-0.2
10	0.5	9.5	12.3	2.8	12.3	0.5	2.8
20	0.4	19.6	22.8	3.2	22.8	0.4	3.2
...	...	...	...	...	...	...	...

3.5 Application of Angular Errors

Now suppose we want to use the above results to measure an unknown wind direction with an independent anemometer and in an environment where there is no perturbation error. Without loss of generality we assume there is no systematic anemometer error in this measurement, or at least the systematic error is fully corrected. With self-similarity (and a perfectly scaled ship model) we now have the equivalent of measuring the wind direction at sea.

Let w" be the observed wind angle in the WITH SHIP case (Figure 2c). In the NO SHIP case the direction of the wind is t (no perturbing influences). The effect of the perturbing influences in the real wind tunnel NO SHIP test is to rotate the wind direction by -e. A plausible statement that the perturbing influences are in some sense the same in the real wind tunnel NO SHIP and WITH SHIP tests is that the wind directions are both rotated by the same perturbation error e. Equivalently, the angular error E is assumed to be the same in the perturbation-free case.

From Figure 2c

$$w + e = w'' - E = w' + e - E = t. \qquad (11)$$

The problem is to find $t(w'')$, given w'' and the wind tunnel tables. Noting that

$$\begin{aligned} w'' &= w' + e \\ &= n' + p \end{aligned} \qquad (12)$$

the solution is to regard $w'' = n' + p$ as the independent variable, E as the dependent variable and accordingly construct lookup tables from the wind tunnel data. The wind direction is then obtained by looking up the angular error E corresponding to w'', interpolating as required, and subtracting from w''. $E(w'')$ is the sought-for error function to be subtracted from wind direction observations. We emphasize that the probe systematic error drops out in the final results. Table 3 is an example of such a lookup table, derived from the data presented in Table 2.

Table 3. Partial lookup table for Dawson angular errors

$w'' = n' + p$	$E(w'')$
...	...
-20.7	-0.7
-11.0	-1.0
-0.2	-0.2
12.8	2.8
23.2	3.2
...	...

A friendlier table can be constructed by linearly interpolating $E(w'')$ to values of w'' that are multiples of 10 degrees, changing the sign of $E(w'')$, and then adding 360 degrees to the negative w'' values. This was done for both anemometer locations on the three ships. The results are

presented in Tables 5, 6, and 7 for the Dawson, Baffin, and Hudson, respectively. Column 1 gives w" at regular 10 degree increments, column 2 gives the interpolated values of -E(w") for the regular anemometer location, and column 4 gives -E(w") for the bow anemometer.

3.6 Speed Measurements

The NO SHIP wind speed at the location to be occupied by a shipborne anemometer when the ship is present, measured by the miniature cylindrical probes, is labeled V_r. For each test sequence, the ratio of speeds V_r/V_g is recorded for each value of turntable angle t.

In the WITH SHIP tests, let the observed speed in the free stream be V_g' while the observed disturbed speed at the ship anemometer location be V'. Note that V_g' may be different from the NO SHIP V_g since the tests are conducted at different times and there might be some effect on Vg' even at the same fan power due to the blockage caused by the ship model in the wind tunnel.

The quantity of ultimate interest in the WITH SHIP tests is the speed correction function

$$R = V'/V_r' \tag{13}$$

where V_r' is the wind speed that would be seen at the ship anemometer location in the current test sequence if no ship were present but the free stream speed were the same. As pointed out in Section 3.2 it is a simple matter to invoke self-similarity to infer the correct value of V_r' from

$$V_r'/V_g' = V_r/V_g, \tag{14}$$

and obtain R as the ratio of speed ratios for each value of t:

$$R = (V'/V_g') \; / \; (V_r/V_g). \tag{15}$$

In SEM, R is called "Observed Speed/Reference Speed". Note that this use of speed ratios (i) compensates for any variation in the free stream speed, (ii) eliminates any constant multiplicative systematic errors in the speed probes, and (iii) eliminates any multiplicative speed perturbation errors, assuming that, as for the (angular) perturbation errors, they are the same for corresponding NO SHIP and WITH SHIP tests. Such errors would exactly cancel between the two ratios. Errors (ii) and (iii) are the speed analogues of the angular errors a and e, respectively.

Thus each test sequence results in a table of values of R as a function of t. SEM chose to eliminate t between n(t) and R(t) and produced display tables and plots giving R as a function of n rather than n', the WITH SHIP observed angle, as was done for the angular errors. Table 4 illustrates this procedure with a portion of the same Dawson test sequence used in Table 2.

Table 4. Partial test sequence results for Dawson (speed measurements)

Measurements		Display Table	
t	R(t)	n	R(n)
...	...	...	...
-20	1.07	-19.7	1.07
-10	1.07	-9.5	1.07
0	1.07	1.0	1.07
10	1.08	9.5	1.08
20	1.10	19.6	1.10
...	...	...	...

3.7 Application of Speed Correction Functions

We now use the above results to determine an unknown wind speed with an independent systematic-error-free anemometer in a perturbation-free environment. Just as for direction measurements, we are treating the equivalent of measuring the wind speed at sea. Let the observed disturbed speed be $V"$ (at observed direction $w"$). Let the corresponding undisturbed speed be $V_r"(w")$, the unknown speed or corrected version of $V"(w")$ that we wish to find. If we have already gone through the exercise of determining $E(w")$ and $t(w")$, we could use Table 4 to look up the corresponding $R(t)$, interpolating as required. Since R is free of anemometer-specific systematic errors and perturbation errors, it applies as well to the current measurement and we have

$$V_r"(w") = V"(w") \; / \; R[t(w")], \tag{16}$$

showing how the speed correction function is applied to wind speed measurements.

Again a friendlier table was constructed by linearly interpolating $R[t(w")]$ to values of $w"$ that are multiples of 10 degrees, forming the reciprocals, and appending columns for the reciprocal speed correction functions to Tables 5, 6, and 7. Columns 3 and 5 list interpolated values of $1/R[t(w")]$ for the regular and bow anemometer locations, respectively. All data presented in these tables was derived from the basic set of test sequences defined in Section 3.1.

3.8 Wind Tunnel Blockage

Wind tunnel blockage is the name given to the restraining effect of the walls and ceiling on the flow streamlines that might otherwise have curvature around a model in the wind tunnel. The effect applies to the model plane as well as to the downstream wake. There is experimental evidence (D. Surry, private communication) that for bluff bodies the effect on wind speed can be non-negligible, particularly in boundary layer flow. Blockage effects have been formulated as corrections for overall drag and for pressure. Most of the bluff body drag formulations give a correction

for the speed squared of 2 to 2.5 times the area ratio (e.g., Melbourne, 1982). For example, the Dawson model which is the largest of the three tested, presents an area ratio of 2.5% in BLWT II when broadside to the wind. In this worst case, the speed error due to wind tunnel blockage then overestimates the unrestrained wind by as much as 3 percent.

A rule of thumb in wind tunnel operations is that blockage for streamlined bodies in uniform flow is negligible for area ratios below 5%. For two-dimensional bodies, the effect on speed is of the order $\pi^2/12$ times the square of the area ratio (Pope, 1954). The speed correction for this type of wind tunnel blockage due to an area ratio equal to the Dawson worst case is then less than 0.1 %. However, the bluff body correction would seem to be the more applicable one for ship models.

No adjustment was made in SEM or this report for blockage errors. It should be noted that the reported Dawson speed correction functions for broadside winds differ from unity by 6 to 8 %. Hence a 3% overestimate could account for a substantial part of the reported corrections.

4. WIND TUNNEL RESULTS

4.1 Displayed Correction Functions

Figures 3 - 6 exhibit the correction functions for the basic set of tests. The remaining figures pertain to the additional test sequences carried out on the Dawson. The vertical profile tests are contrasted in Figs. 7 - 10, the rolled and pitched orientation tests are displayed in Figs. 11 - 18, while the bow anemometer height tests are contrasted in Figs. 19-20.

4.2 Symmetries

The near symmetry of most ships about a vertical plane through the ship axis is expected to produce two types of symmetries in the displayed functions $E(n')$ and $R(n)$ principally for the bow anemometer (which is located on the plane of symmetry) but also showing some traces for the regular anemometer. For a level symmetric ship we expect

$$E(n') = -E(-n') \tag{17}$$

and

$$R(n) = R(-n), \tag{18}$$

while for rolled orientations

$$E_p(n') = -E_s(-n') \tag{19}$$

and

$$R_p(n) = R_s(-n), \tag{20}$$

where subscripts p and s refer to the 20 degree roll to port and starboard tests, respectively. Note that it is immaterial whether the independent variable is n or n' in any one of these symmetry statements.

Examples of eq (17) are found in Figure 5. In addition to the odd symmetry of the angular error which is clearly apparent for each ship, the data plots show a uniform sinusoidal shape in the forward 240 degrees with amplitudes of about +/-6 degrees at +/-60 degrees. Examples of eq (18) are found in Figure 6, showing the even symmetry of $R(n)$ for the three ships. Again there is marked uniformity among the ships. The speed ratio is a few percent less than 1.0 for bow winds, then rises to a broad maximum of about 1.1 for 90 degree winds. An example of eq (19) is seen in the port and starboard roll plots in Figure 15. A reflection of one set of data points through the origin produces a set very similar to the other. Finally an example of eq (20) is seen in the port and starboard roll plots in Figure 16 in which a reflection of one figure about the vertical axis is very similar to the other.

4.3 Regular Anemometer Experiments

4.3.1 Angular Errors

The basic set of experiments for the regular anemometer location reveals some interesting differences, especially for angular errors, and yet some similarities among the ships. Plots of E(n') (Figure 3) show a faint resemblance to the odd-symmetric bow anemometer plots. For starboard winds a principal deviation from the bow plots is the rapid change of angular error centered at about 90 degrees due to the mast wake. The mast wake deviation goes through a full cycle with an amplitude of about 4 degrees for the Dawson and about 6 degrees for the Baffin and Hudson. The deviation affects a narrower range of wind directions for the Dawson (about 40 degrees) than the other ships (about 60 degrees for both Baffin and Hudson).

For winds over the port side the angular error for the Hudson regular anemometer bears the closest resemblance to that for the bow anemometer. The sinusoidal form and amplitudes are nearly the same except understandably for stern winds. An explanation of this feature might be that the regular anemometer on the Hudson is relatively closer to the bow than for the other ships, and relatively higher above the superstructure, especially in comparison to the Baffin. The port side angular errors for the Dawson and Baffin are negative as for the bow, but comparatively small in magnitude, averaging about -3 degrees.

4.3.2 Speed Correction Functions

Speed corrections at the regular anemometer sites for the three ships are displayed in Figure 4. The display function R(n) is greater than 1.0 by at most 12% over much of the starboard range and undergoes a sharp dip in the mast wake, especially pronounced for the Baffin and Hudson where it reaches a low of 0.65. The corresponding Dawson dip goes down to 0.85.

For port winds R(n) is very close to and never less than 1.0. The speed correction function is nearly constant at about 1.05 for the Hudson.

More variation of the function is seen for the Dawson and Baffin. The Dawson has a wide range of port directions for which R(n) hovers around 1.07, while the Baffin values are generally closer to 1.0.

4.3.3 Discussion

Except for the location and magnitude of the starboard dip, the correction functions for the regular anemometers of the three ships are seen to be relatively smooth functions, similar in form, and close in magnitude.

The angular errors at the bow on the Baffin and Hudson show peculiar asymmetric fluctuations at wind directions in the neighborhood of 20 degrees, apparent in Figure 5. Examination of the deck apparatus and structures near the bow on both models shows there is a high degree of symmetry, suggesting the fluctuations may be fortuitous. A possible explanation may be related to the perturbation caused by the wake of a supporting post near both bow anemometers, and the perturbation caused by the bow probe wake on the probe at the regular anemometer site occur at angles in this neighborhood. Although compensation has been applied for perturbation effects it may be that the method is not always satisfactory. That the same behavior is seen at the same position for the regular anemometers (Figure 3) reinforces this conjecture. On the other hand if this is the correct explanation why does it not apply to the Dawson angular errors which show only very slight fluctuations in this direction? It is suggested in SEM that the self-aligning fairings on the vertical posts may not have performed consistently from one experiment to another.

4.4 Additional Dawson Experiments

4.4.1 Vertical Wind Profile Experiments

In the progression of vertical wind profiles from smooth to rougher to roughest some trends are seen for the Dawson. For the regular anemometer site, the angular error (Figure 7) remains very similar in overall shape and amplitude except that there is an appreciable reduction in the size of the deviation in the mast shadow. The speed correction function (Figure 8) also remains very nearly the same except for the growth with increasing roughness of small amplitude wiggles and the interesting onset of a symmetrically located dip when the regular anemometer is approximately upstream of the mast.

In the same progression of tests for the Dawson bow anemometer, the correction functions show little change (Figures 9 and 10). The angular error remains very nearly the same, while small amplitude wiggles develop in the speed correction function.

4.4.2 Pitch Experiments

The progression of 5 degree pitch tests from bow down to level to bow up reveal some interesting trends. Only the half-azimuth (starboard) winds were examined in the pitch tests. Three characteristics are noted for the angular errors at the regular anemometer site (Figure 13): (1) for near-bow winds the rate of change of the angular error with direction increases appreciably from about 0.1 to 0.3 degree per degree as the bow rises; (2) the mast shadow effect decreases slightly in amplitude; (3) no appreciable or uniform change is seen in following winds. Corresponding characteristics are noted for the speed correction functions (Figure 14): (1) an anomalous dip appears just off the bow when the bow is pitched up, but otherwise there is little change in forward winds; (2) the location of the mast shadow dip shifts from about 80 to 95 degrees; (3) no appreciable or uniform change is seen in following winds.

Angular errors at the bow anemometer site retain the same sinusoidal form (Figure 17). One notable change is that the positive-to-negative crossover point shifts forward from 115 to 90 degrees. The speed correction function shows a nearly uniform increase of a few percent and some irregularities in the pitched positions (Figure 18).

4.4.3 Roll Experiments

The progression of 20 degree roll tests from port to level to starboard was carried out for the full-azimuth range. Angular errors at the regular anemometer site, displayed in Figure 11, show the following changes: (1) for starboard winds, as the ship rolls from port toward the wind, the angular error retains approximately the same sinusoidal form but decreases dramatically in amplitude from about 10 to 4 degrees, while the mast shadow fluctuation virtually disappears; (2) for port winds, the angular error displays an approximate sinusoidal form that undergoes a sign reversal, especially clear for the near-bow winds. The corresponding speed correction errors, displayed in Figure 12, show the following changes: (1) for starboard winds, as the ship rolls toward the wind, the mast shadow dip changes from a very broad and prominent feature to a minor effect; (2) for port winds, the speed correction shows a small increase from values generally slightly less than 1.0 to values around 1.1.

Comments on the angle and speed correction functions for the bow anemometer roll tests with respect to one of the two types of symmetries were already made. Here we note a few other characteristics apparent in Figures 15 and 16: (1) the level ship functions occupy an intermediate position between those of the two extreme rolled positions for directions up to 60 degrees off the bow; (2) the rate of change of angular error for bow winds seems surprisingly large (0.2 degree per degree) and is even larger (0.25 degree per degree) at the two rolled positions; (3) regarded as approximate sine curves, the amplitudes of the angular error functions for the two rolled positions are also surprisingly large (10 degrees) and nearly twice as large as the level

ship function; (4) there is a shift of the angular error curves toward the direction of the roll; (5) in comparison to the level ship the rolled ship speed correction functions are more nearly 1.0 over most of the range of wind directions from the side toward which the ship is rolled.

4.4.4 Bow Anemometer Height Experiments

The final set of special Dawson experiments investigated the effect of varying the bow anemometer height. The three above-waterline heights were 11.5, 12.5, and 14.5 m. The angular errors and speed correction functions are displayed in Figure 19 and 20, respectively. These were starboard wind tests only since symmetry about the ship axis was expected. The angular errors for 11.5 and 12.5 meters are nearly the same, especially for directions forward of the positive-to-negative crossover point at 100 degrees. The 14.5 m height gives appreciably smaller errors for this same forward range. The speed correction functions show an irregular behavior with height, but generally the 14.5 m anemometer gives speed corrections closest to 1.0, while the 12.5 m height curiously gives the largest corrections in a broad middle range of angles (30 to 130 degrees).

5. SUMMARY, CONCLUSIONS AND DISCUSSION

The wind tunnel experiments give correction functions for the regular shipboard anemometers and proposed bow anemometers for the C.S.S. Dawson, C.S.S. Baffin, and C.S.S. Hudson. The functions apply most accurately to ships at rest in the water. The applicable wind speed range may be ambiguous. If self-similarity is in force, as boundary-layer wind-tunnel experience supports, the applicable marine wind profile corresponds to 10 meter height speeds in the range of 15 to 30 m/s in a neutrally stable atomospheric boundary layer. On the other hand, Reynolds number scaling would make these results apply to very low wind speeds. To use the functions displayed in the summary figures taken from SEM and presented in this report is awkward because information must be scaled graphically from the figures and because the treatment of perturbations is not straightforward. Tables 5, 6, and 7 were prepared to simplify the task of

of making corrections. All directions are relative to the ship's heading. The OBSERVED DIRECTION is located in the left hand column. The tabulated ANGULAR CORRECTION is then read off and added to the OBSERVED DIRECTION to get the correct direction. The correct speed is obtained by multiplying the observed speed by the tabulated SPEED FACTOR.

An inspection of Figure 5 reveals that in the vicinities of +/- 140 degrees the Baffin angular error at the bow anemometer site undergoes large negative incremental changes as a function of observed angle. When such changes are larger than 10 degrees, the angular error branches into a three-valued function of w". In other words there are some observed wind directions for which the correct directions, having two or three possible solutions (as for a cubic equation), are indeterminate. Only one of these cases is picked up by the 10 degree steps in Table 6 and is indicated by a "?".

The additional tests run on the Dawson permit applying corrections to a wider range of conditions. Optimum use of the pitch and roll functions would necessitate automated corrections with input from the ship's gyrocompass. Information only about the average state of motion as inferred from qualitative information on the sea state could still be usefully employed as input to the pitch and roll functions.

How best to make at least a crude correction for the ship velocity is not clear. Should one add the ship velocity to the anemometer velocity or to the corrected velocity? A simple argument applied to a symmetrically placed anemometer on a symmetric ship suggests an answer. Compare case (a) of a ship moving at 10 knots in a dead calm to case (b) of a ship at rest with a 10 knot wind over the bow. The argument depends on the conjecture that in both cases an accelerated wind speed would be observed but the increase in case (a) is greater than in (b) since more air is moving around the ship. Applying the speed correction factor determined from case (b) to the anemometer speed observed in case (a) and then adding the ship speed is the favored method since it results in a smaller error than if the ship speed is added before applying the speed correction.

The original reason for investigating a bow anemometer was the expectation that smaller errors would be found. This is generally true but there are still appreciable errors. The virtue of a bow anemometer appears now to be that the correction functions are smoother and more predictable among different ship architectures. Smoother functions are characterized by fewer parameters. A few well-chosen experimental measurements for a representative member of each class of ship would determine the correction functions.

6. ACKNOWLEDGEMENTS

We wish to thank the Scientific Authority, Bob Anderson (BIO), for his support and encouragement of this project. Helpful comments and support from Fred Dobson (BIO) and Stu Smith (BIO) are also much appreciated. Stu's critical reading of the manuscript led to invaluable improvements in the readability and utility of the final report.

The author wishes to thank Boundary Layer Wind Tunnel Laboratory personnel for their kind hospitality during his visits to their facilities. Special thanks are due Dave Surry and Tom Edey at BLWTL for their initiatives and cooperative involvement in the project and their efforts in clarifying many aspects of the wind tunnel experiments.

We are grateful to Don Dinn and John Parsons (Marine Services, BIO) who authorized our use of the models of the C.S.S. Dawson, C.S.S. Baffin, and C.S.S. Hudson. Jim Dockrill (Marine Services, BIO) was very helpful in handling the models and providing blueprints.

This work was performed under contract OSC88-00005(012) issued by Supply and Services Canada under the Unsolicited Proposal Program and received funding support from the Unsolicited Proposal Fund. Funding support from the Department of Fisheries and Oceans and from the Atmospheric Environment Service is also acknowledged.

This project was partially funded by the Federal Panel on Energy Research and Development, Department of Energy, Mines and Resources.

7. REFERENCES

Anderson, R.J., 1990: manuscript in preparation.

Blanc, T.V., 1986a: The Effect of Inaccuracies in Weather-Ship Data on Bulk-Derived Estimates of Flux, Stability and Sea-Surface Roughness, J. Atmos. and Oceanic Tech., 3, pp. 12-26.

Blanc, T.V., 1986b: Superstructure Flow Distortion Corrections for Wind Speed and Direction Measurements made from Tarawa Class (LHA1-LHA5) Ships, U.S. Naval Research Laboratory, Report 9005.

Charnock, H., 1955: Wind Stress on a Water Surface, Quart. J. Roy. Meteor. Soc., 81, pp. 639-640.

Dobson, F.W., 1981: Review of Reference Height for and Averaging Time of Surface Wind Measurements at Sea, World Meteorological Organization, Marine Meteorology and Related Oceanographic Activities, Report No. 3, 64 pp.

Kendall, M.G. and A. Stuart, 1961: The Advanced Theory of Statistics, Vol. 2, Charles Griffin & Co., Ltd., London, p. 79.

Melbourne, W.H., 1982: Wind Tunnel Modeling for Civil Engineering Applications, Proc. of Workshop at Gaithesburg, Maryland, April, Cambridge U. Press.

Pope, A., 1954: Wind-Tunnel Testing, 2nd edition, John Wiley & Sons, Inc., New York, p. 278.

Romanov, Yu.A., I.B. Fedorova, M.S. Chervyakov, and G.I. Shapiro, 1983: An Improvement in the Accuracy of Shipboard Measurements of Wind Speed and Direction Based on Aerodynamic Tests of a Ship Model, Oceanology, 23, No. 2, pp. 267-270.

Smith, S.D., 1981: Coefficients for Sea-Surface Wind Stress and Heat Exchange, Rep. BI-R-81-19, 31 pp., Bedford Inst. of Oceanogr., Dartmouth, N.S.,Canada.

Smith, S.D., 1988: Coefficients for Sea Surface Wind Stress, Heat Flux, and Wind Profiles as a Function of Wind Speed and Temperature, J. Geophys. Res., 93, C12, pp. 15,467-15,472.

Surry, D., R.T. Edey, and I.S. Murley, 1989: Speed and Direction Correction Factors for Shipborne Anemometers, University of Western Ontario, Boundary Layer Wind Tunnel Report, BLWT-SS9-89.

Surry, D., A. McDougall, and I. Murley, 1989: A Miniature Cylindrical Wind Speed and Direction Sensor, Proc. 8th Colloquium on Industrial Aerodynamics, Aachen, W. Germany, Sept 4-7.

Surry, D., A. McDougall, I. Murley, and R.T. Edey, 1990: Calibration of Miniature Cylindrical Pressure Sensors for Determining Mean Wind Speed and Direction, University of Western Ontario, Boundary Layer Wind Tunnel Report, BLWT-SS9-90.

Vickery, P.J., B.J. Vickery, and A.G. Davenport, 1985: Gust Factors and Turbulence Measured at 50 m over the Sea off Sable Island, Proc. Int. Workshop on Offshore Winds and Icing, Halifax, N.S., Canada, pp. 196-213.

Table 5. Anemometer Corrections for C.S.S. Dawson.

(Add ANGULAR CORRECTION to OBSERVED DIRECTION)
(Multipy observed speed by SPEED FACTOR)

	Regular Anemometer		Bow Anemometer (6.5 m above deck)	
OBSERVED DIRECTION (degrees)	ANGULAR CORRECTION (degrees)	SPEED FACTOR	ANGULAR CORRECTION (degrees)	SPEED FACTOR
0	0.2	0.93	0.8	1.01
10	-2.1	0.93	-1.5	1.00
20	-3.2	0.91	-3.1	1.00
30	-3.7	0.90	-4.1	0.99
40	-4.1	0.89	-4.5	0.98
50	-5.0	0.90	-4.4	0.97
60	-5.8	0.90	-4.4	0.96
70	-5.5	0.90	-4.3	0.93
80	-1.9	0.97	-4.1	0.94
90	-4.8	1.07	-3.2	0.93
100	-6.1	1.08	-1.7	0.93
110	-0.4	0.95	-0.2	0.96
120	3.9	0.91	1.6	0.95
130	7.1	0.91	3.5	0.97
140	8.1	0.92	5.5	1.00
150	7.6	0.98	6.7	1.01
160	5.7	1.01	6.6	1.22
170	4.8	1.01	5.0	1.56
180	5.1	1.00	2.5	1.70
190	4.4	0.99	-0.1	1.35
200	3.3	0.98	0.8	1.01
210	2.7	0.96	2.3	0.99
220	2.1	0.94	2.4	0.97
230	2.3	0.94	2.8	0.96
240	2.3	0.95	3.8	0.96
250	1.4	0.93	4.1	0.94
260	1.4	0.95	5.6	0.93
270	3.9	0.95	6.6	0.93
280	3.3	0.93	6.8	0.93
290	1.1	0.93	7.2	0.93
300	1.0	0.93	7.0	0.95
310	1.0	0.93	6.6	0.96
320	1.4	0.92	6.6	0.97
330	1.0	0.92	5.6	0.99
340	0.7	0.93	4.1	1.01
350	0.9	0.93	2.5	1.00

Table 6. Anemometer Corrections for C.S.S. Baffin.

(Add ANGULAR CORRECTION to OBSERVED DIRECTION)
(Multipy observed speed by SPEED FACTOR)

	Regular Anemometer		Bow Anemometer (8.5 m above deck)	
OBSERVED DIRECTION (degrees)	ANGULAR CORRECTION (degrees)	SPEED FACTOR	ANGULAR CORRECTION (degrees)	SPEED FACTOR
0	-0.5	0.95	-1.5	1.06
10	-4.0	0.94	-4.4	1.05
20	-5.4	0.94	-5.7	1.04
30	-5.4	0.94	-5.9	1.03
40	-6.6	0.93	-7.3	1.00
50	-6.8	0.92	-7.1	0.99
60	-6.5	0.93	-7.6	0.97
70	-3.7	0.94	-7.7	0.94
80	2.1	1.13	-7.2	0.94
90	-0.7	1.45	-6.9	0.94
100	-5.0	1.32	-5.4	0.93
110	-7.4	1.13	-3.9	0.94
120	3.3	0.96	-2.8	0.95
130	6.0	0.93	-0.9	0.94
140	7.0	0.94	1.1	1.00
150	6.0	0.96	22.9	4.52
160	4.2	0.96	16.9	5.51
170	2.4	0.96	10.4	6.57
180	0.9	0.98	2.2	6.13
190	0.3	0.98	-6.0	5.75
200	0.5	0.97	-14.2	5.41
210	-0.2	0.97	-22.4	5.11
220	0.2	0.95	?	?
230	1.3	0.98	1.9	0.94
240	2.2	0.98	3.6	0.95
250	2.9	0.99	4.1	0.94
260	2.5	1.00	4.6	0.92
270	2.6	0.99	5.6	0.92
280	2.5	0.99	5.8	0.94
290	2.0	0.97	6.1	0.94
300	2.9	0.95	6.1	0.97
310	3.4	0.95	5.3	0.99
320	3.5	0.93	4.5	0.99
330	3.0	0.94	3.5	1.01
340	1.4	0.94	2.1	1.04
350	-0.1	0.94	0.5	1.05

Table 7. Anemometer Corrections for C.S.S. Hudson.

(Add ANGULAR CORRECTION to OBSERVED DIRECTION)
(Multipy observed speed by SPEED FACTOR)

	Regular Anemometer		Bow Anemometer (8.5 m above deck)	
OBSERVED DIRECTION (degrees)	ANGULAR CORRECTION (degrees)	SPEED FACTOR	ANGULAR CORRECTION (degrees)	SPEED FACTOR
0	1.1	0.94	-1.1	1.01
10	-2.7	0.94	-4.3	1.02
20	-1.8	0.94	-5.1	1.03
30	-2.2	0.94	-5.0	1.01
40	-3.0	0.92	-5.6	1.00
50	-3.3	0.92	-5.2	0.98
60	-3.5	0.92	-5.5	0.95
70	-2.9	0.92	-5.5	0.94
80	1.5	0.96	-5.5	0.93
90	4.1	1.26	-5.3	0.93
100	1.2	1.47	-3.9	0.93
110	-2.7	1.36	-3.1	0.95
120	-1.5	1.12	-1.5	0.96
130	6.5	0.96	-0.8	0.98
140	8.4	0.95	1.6	1.01
150	7.5	0.97	7.0	1.30
160	6.1	0.97	4.6	1.92
170	5.2	0.98	0.0	3.13
180	4.8	0.98	-3.2	3.26
190	5.1	0.98	-0.9	2.75
200	5.7	0.97	-3.3	1.64
210	5.2	0.96	-2.7	1.12
220	4.9	0.95	1.9	0.99
230	6.2	0.95	2.0	0.96
240	8.0	0.95	2.9	0.96
250	8.8	0.97	3.3	0.94
260	9.3	0.95	3.8	0.93
270	8.8	0.95	5.1	0.94
280	7.1	0.97	5.8	0.94
290	6.4	0.96	6.0	0.95
300	5.8	0.95	5.2	0.96
310	4.9	0.95	4.3	0.97
320	4.3	0.94	3.8	0.99
330	3.6	0.94	2.9	1.01
340	2.6	0.93	1.6	1.04
350	2.2	0.93	0.4	1.04

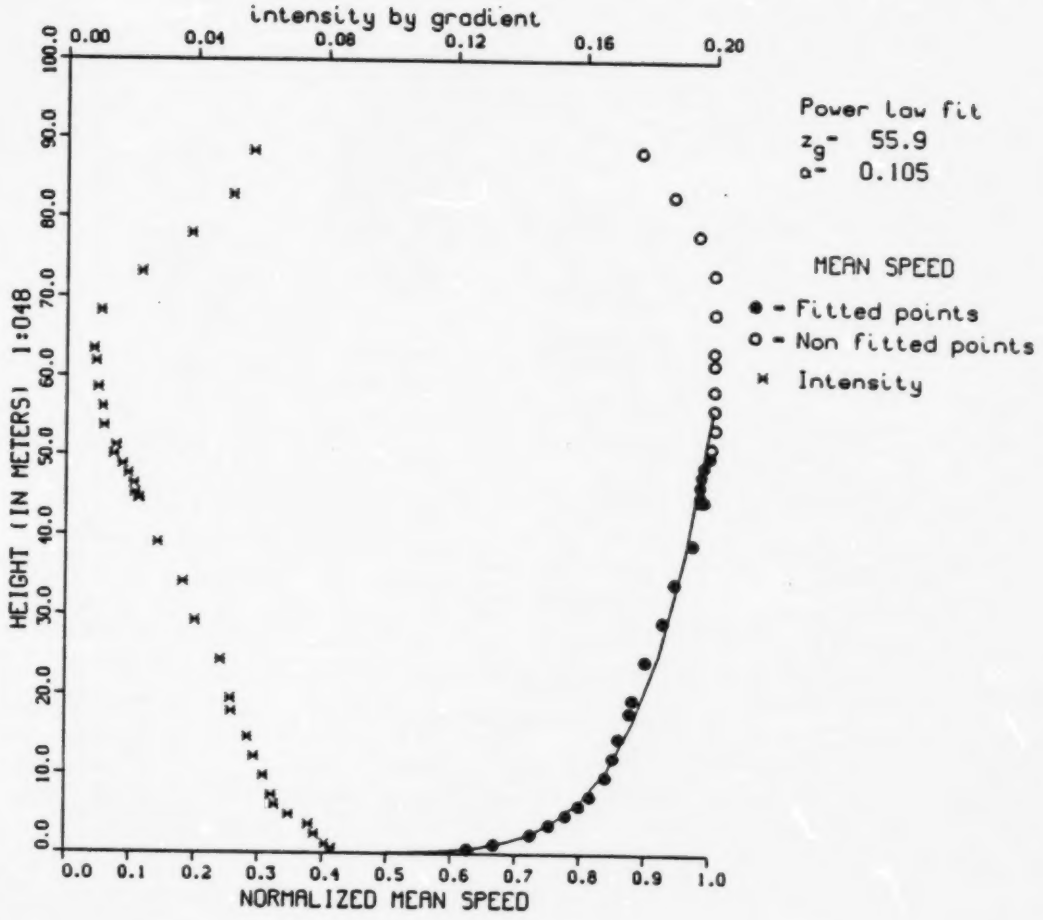

Figure 1. VERTICAL WIND PROFILE - DAWSON - SMOOTH EXPOSURE

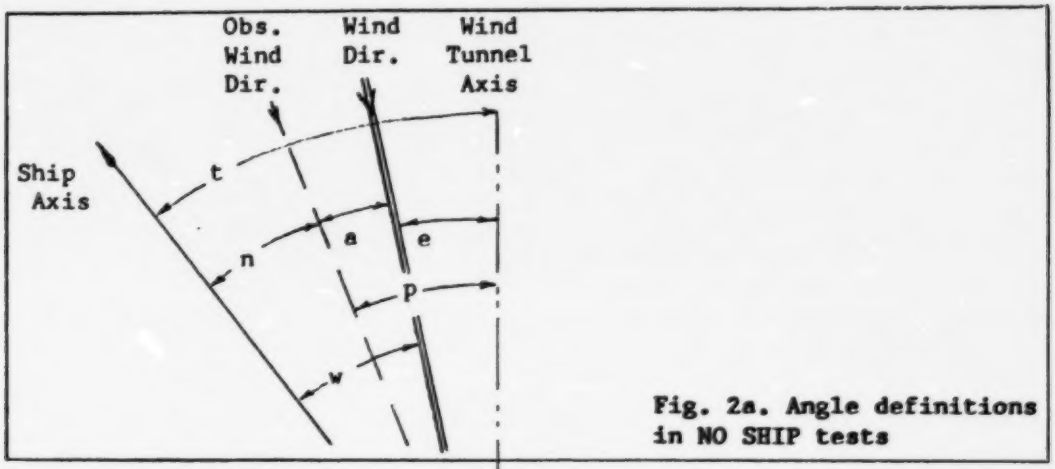

Fig. 2a. Angle definitions in NO SHIP tests

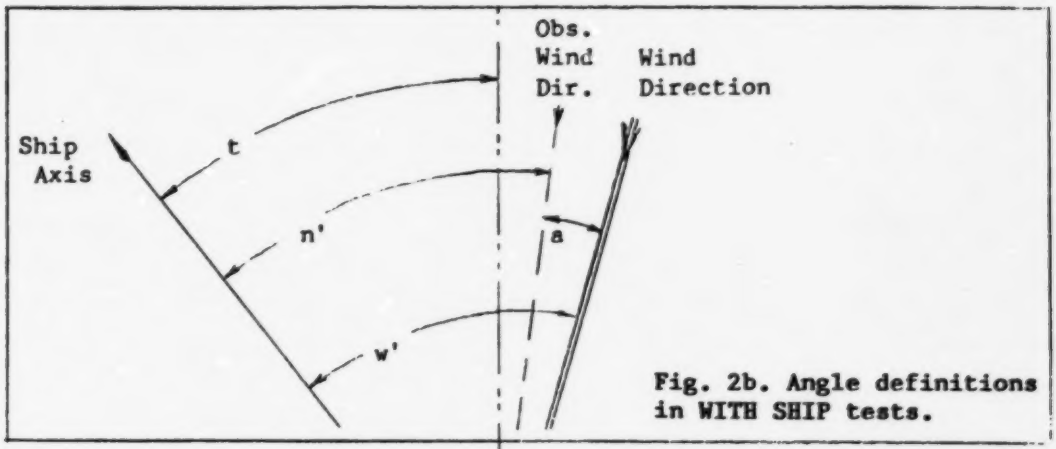

Fig. 2b. Angle definitions in WITH SHIP tests.

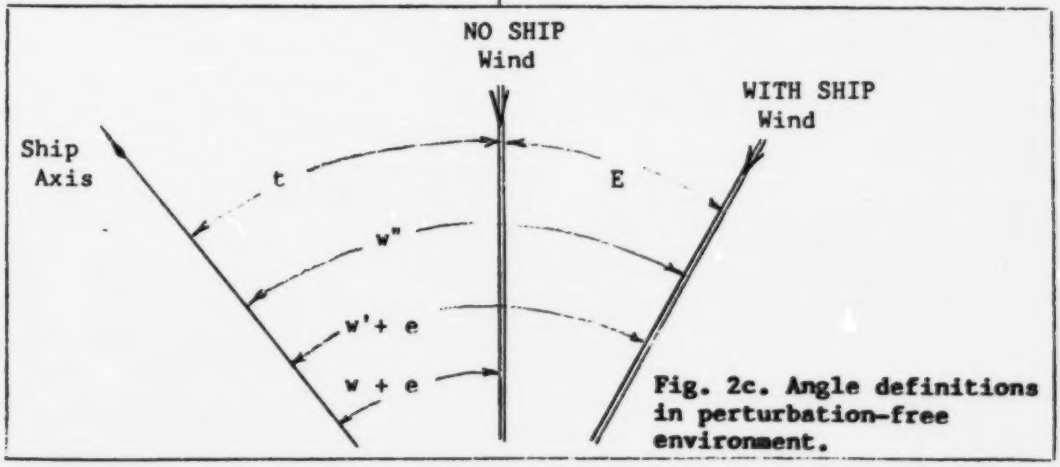

Fig. 2c. Angle definitions in perturbation-free environment.

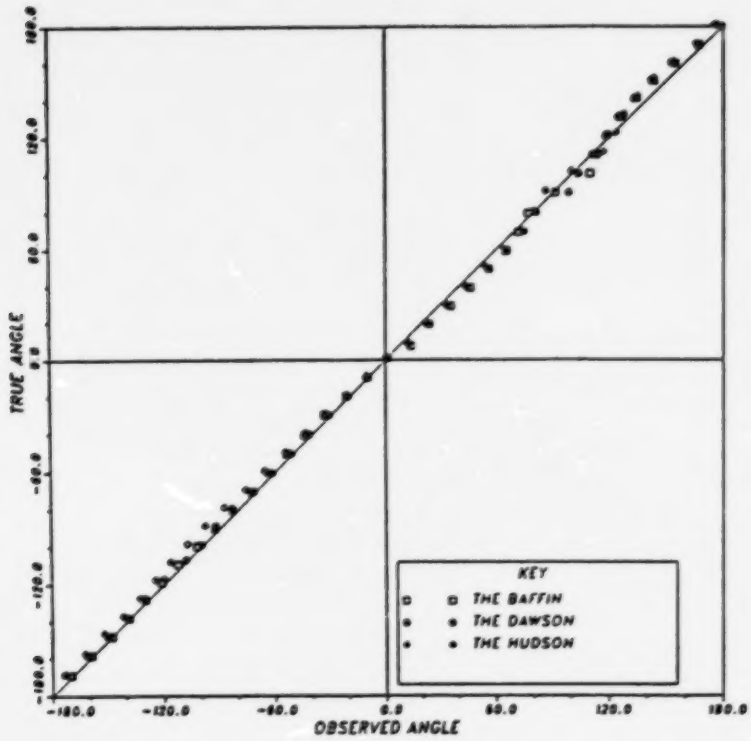

TRUE ANGLE = OBSERVED ANGLE−ANGULAR ERROR

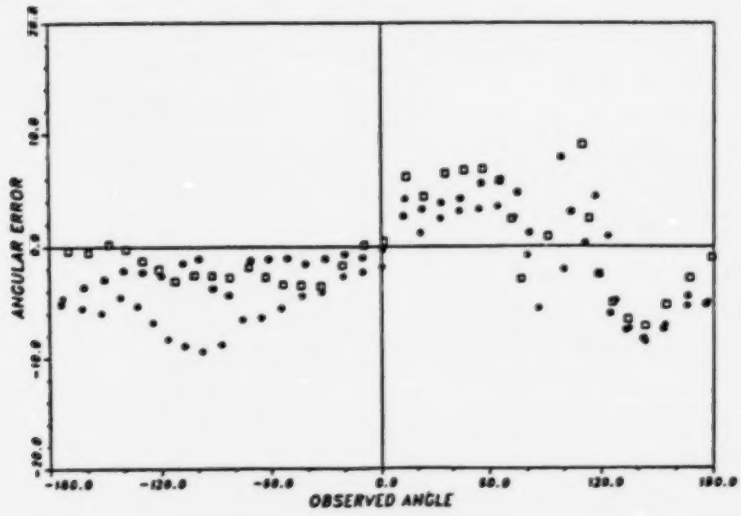

Figure 3. WIND ANGLES FOR ALL SHIPS - REGULAR ANEMOMETER

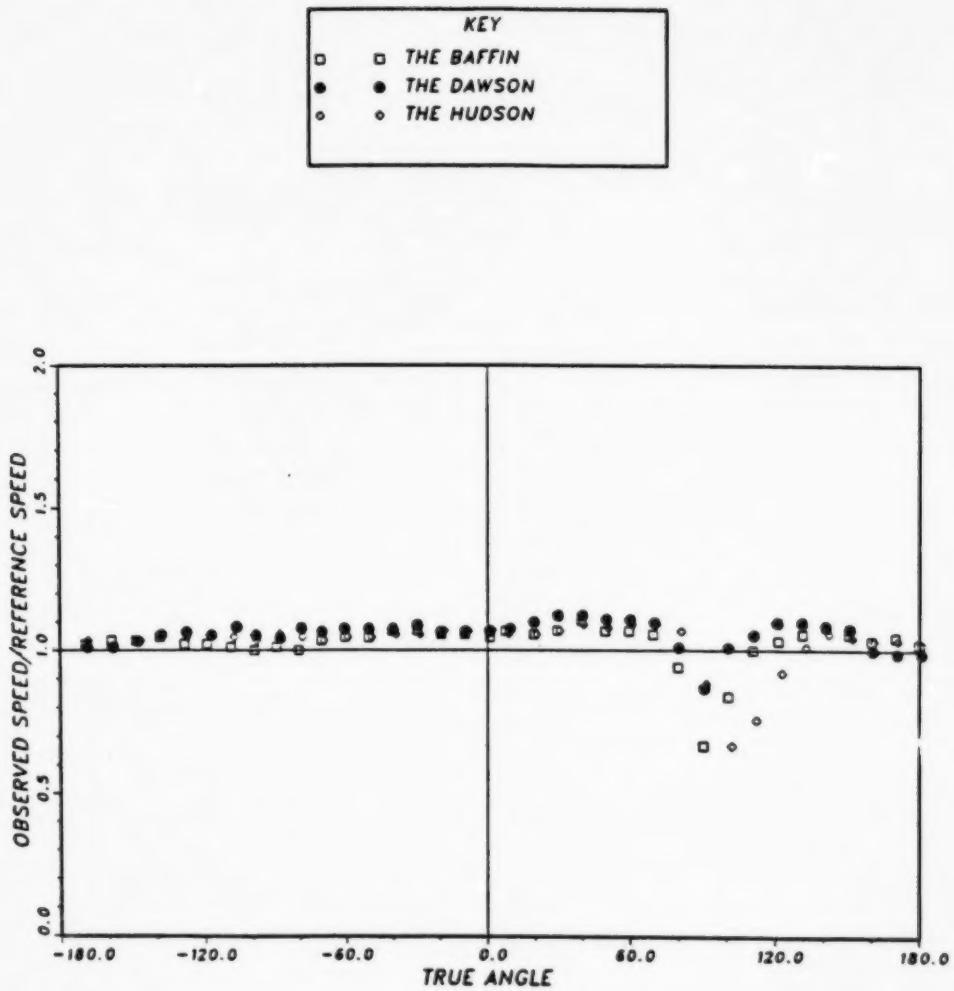

Figure 4. WIND SPEEDS FOR ALL SHIPS - REGULAR ANEMOMETER

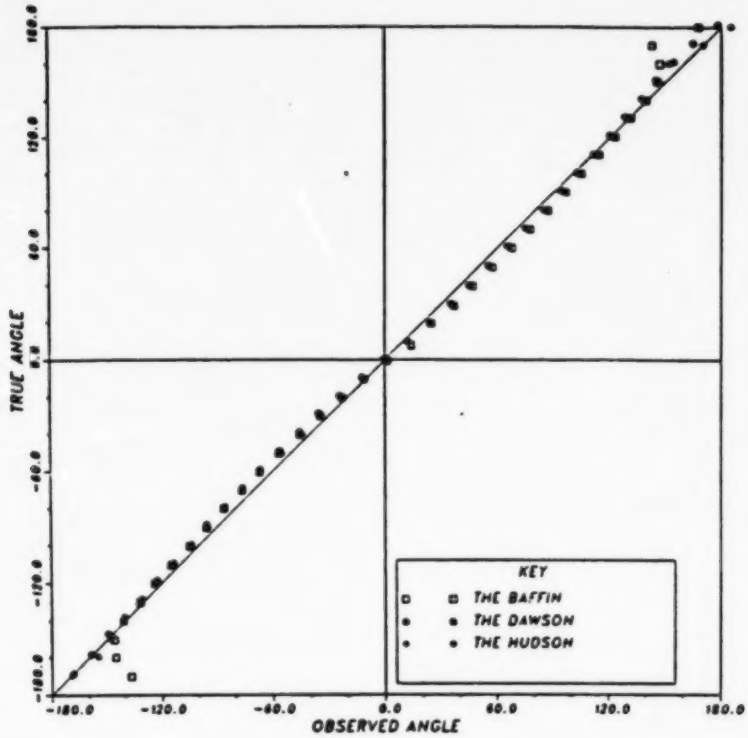

TRUE ANGLE = OBSERVED ANGLE−ANGULAR ERROR

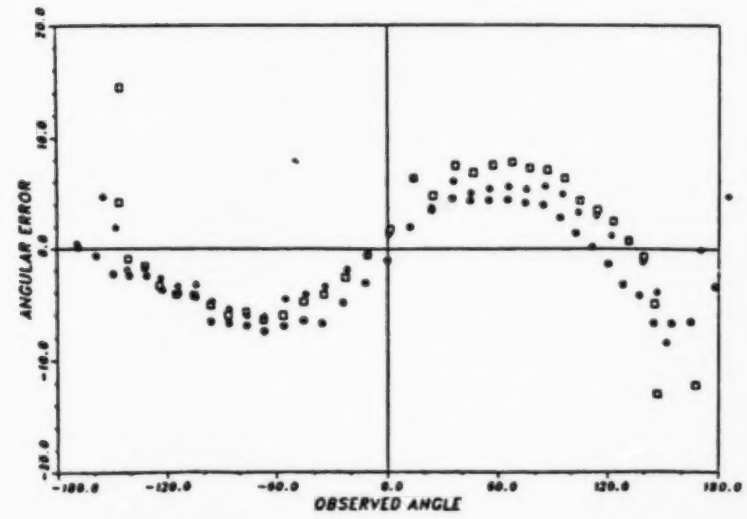

Figure 5. WIND ANGLES FOR ALL SHIPS - BOW ANEMOMETER

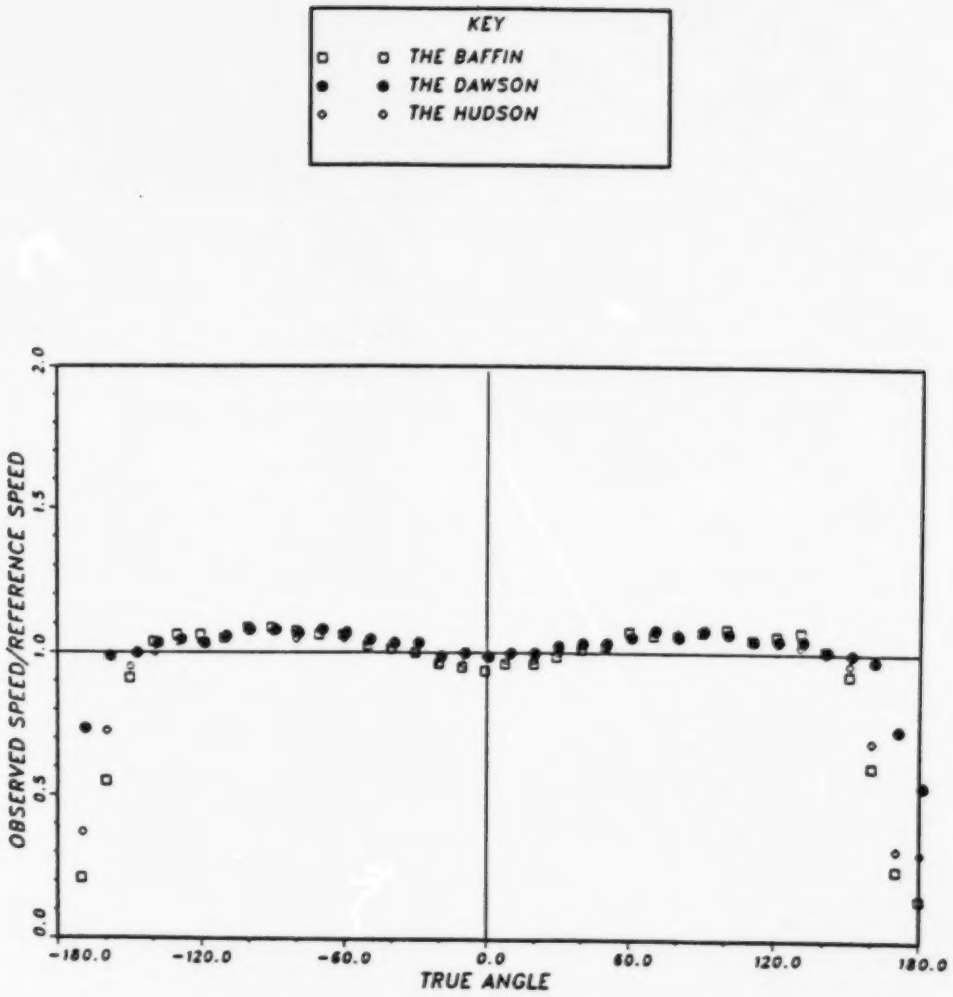

Figure 6. WIND SPEEDS FOR ALL SHIPS - BOW ANEMOMETER

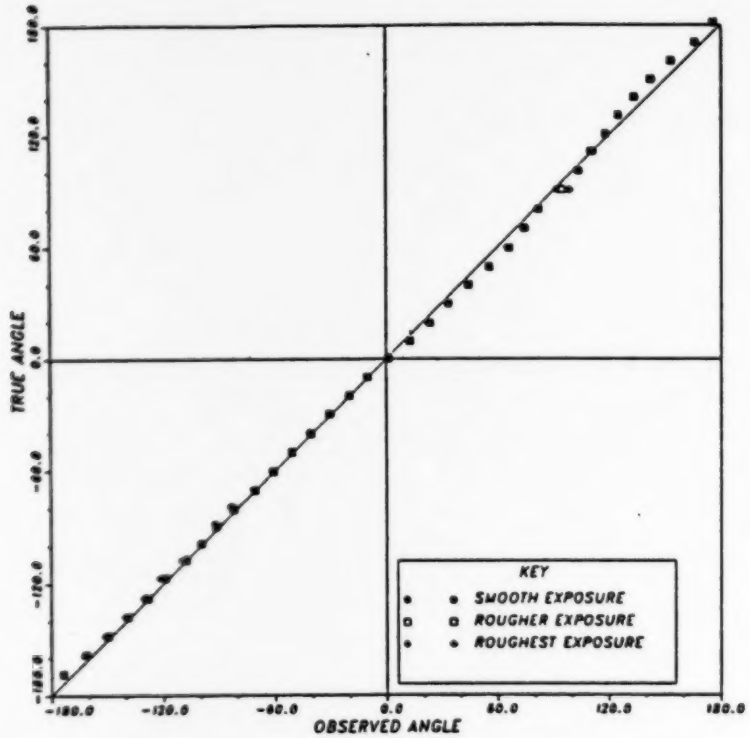

TRUE ANGLE = OBSERVED ANGLE−ANGULAR ERROR

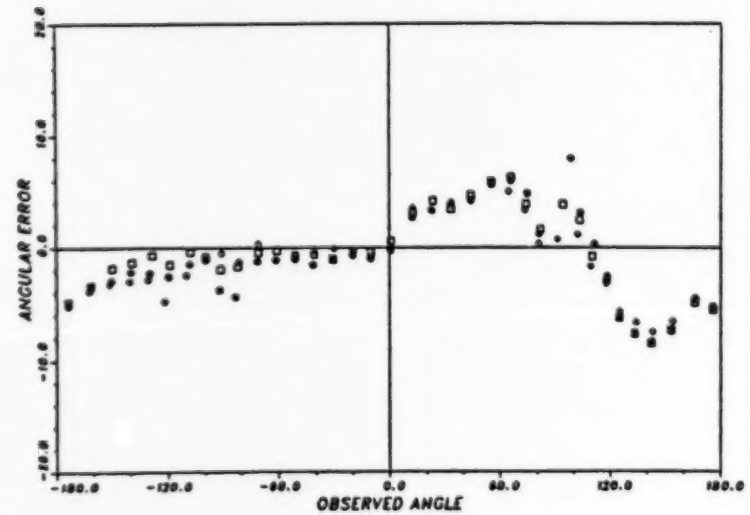

Figure 7. DAWSON WIND ANGLES FOR ALL EXPOSURES - REGULAR ANEMOMETER

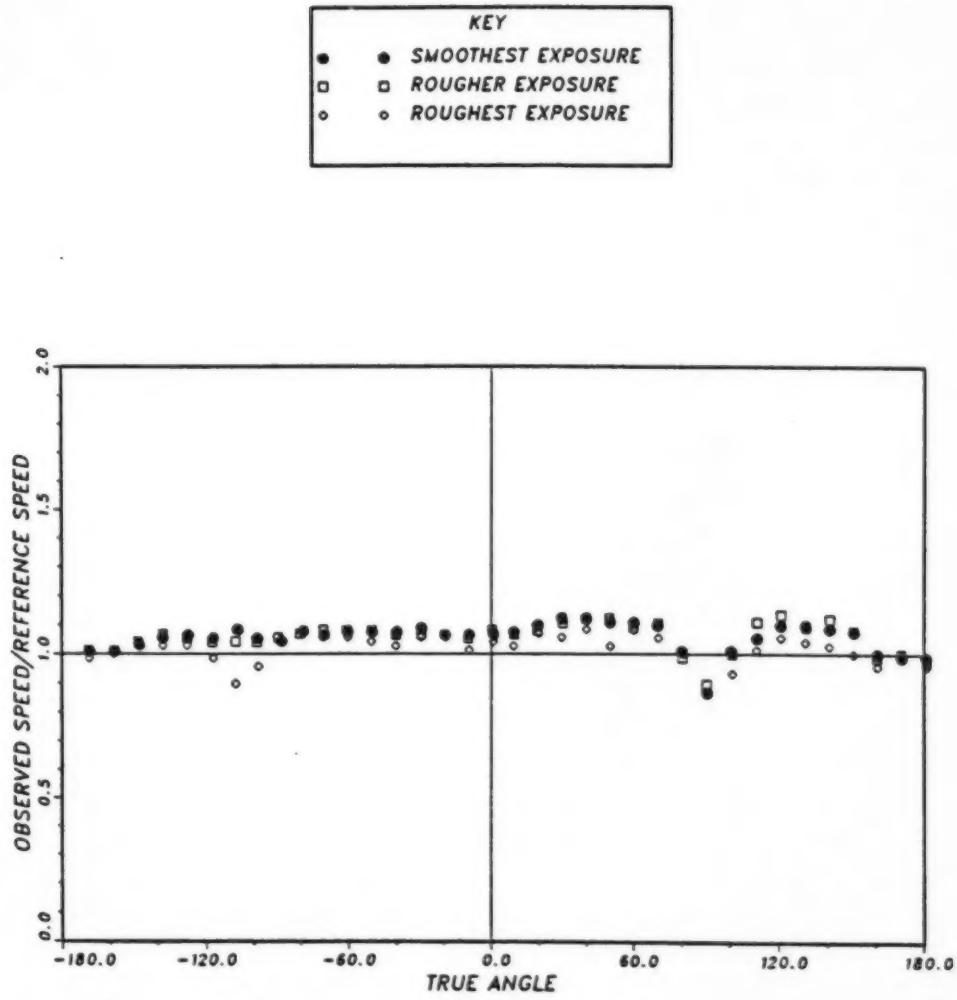

Figure 8. DAWSON WIND SPEEDS FOR ALL EXPOSURES - REGULAR ANEMOMETER

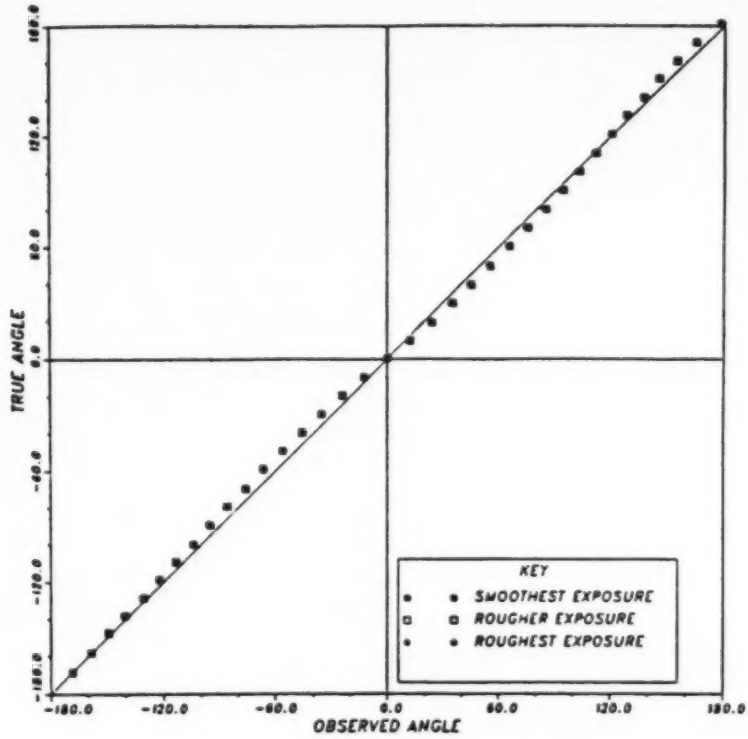

TRUE ANGLE = OBSERVED ANGLE−ANGULAR ERROR

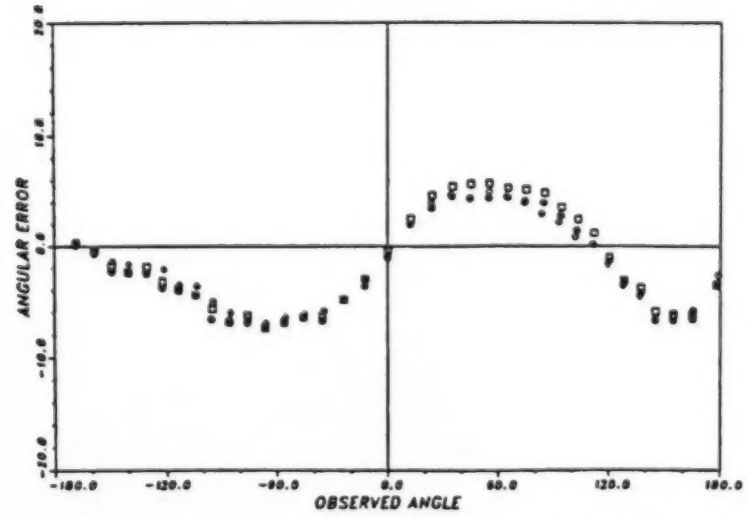

Figure 9. DAWSON WIND ANGLES FOR ALL EXPOSURES - BOW ANEMOMETER

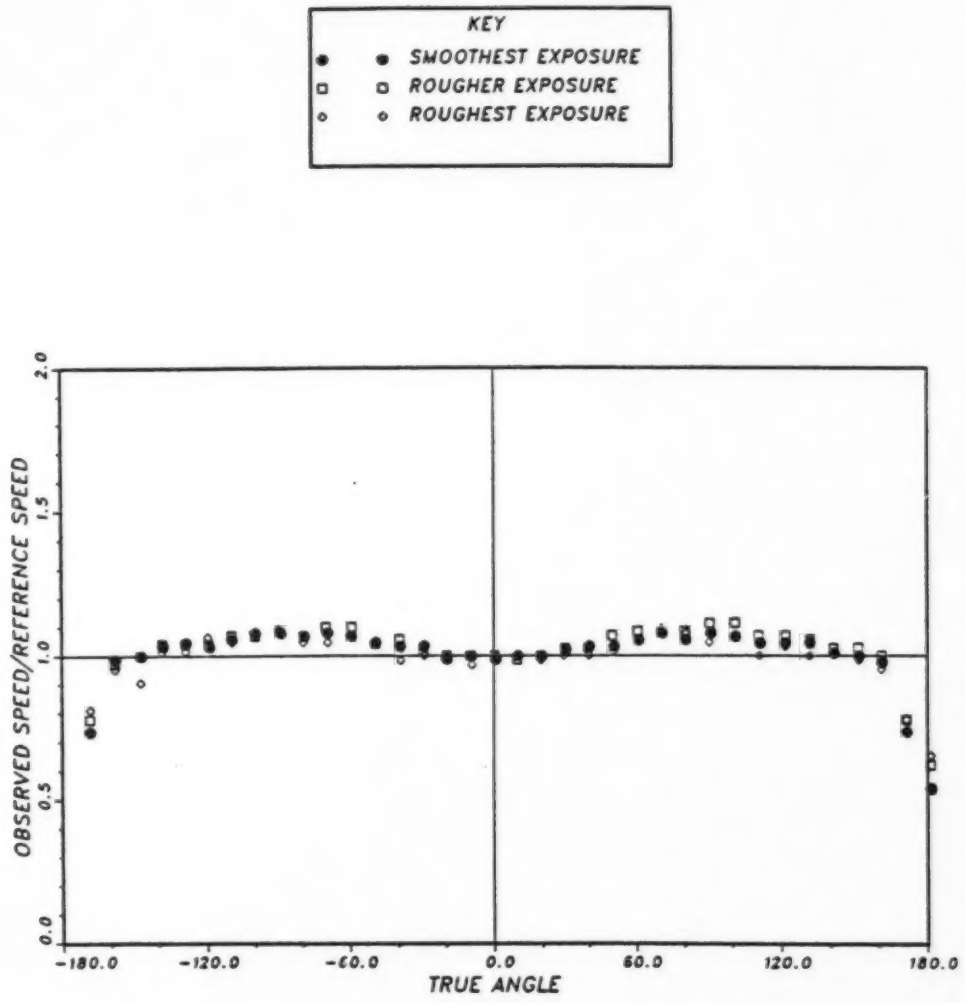

Figure 10. DAWSON WIND SPEEDS FOR ALL EXPOSURES - BOW ANEMOMETER

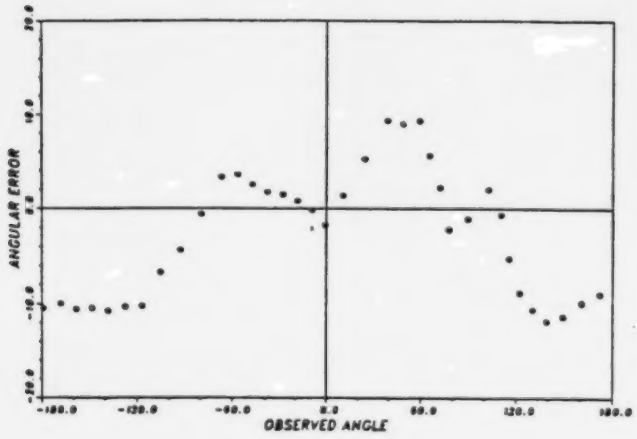

20 DEGREES
TO PORT

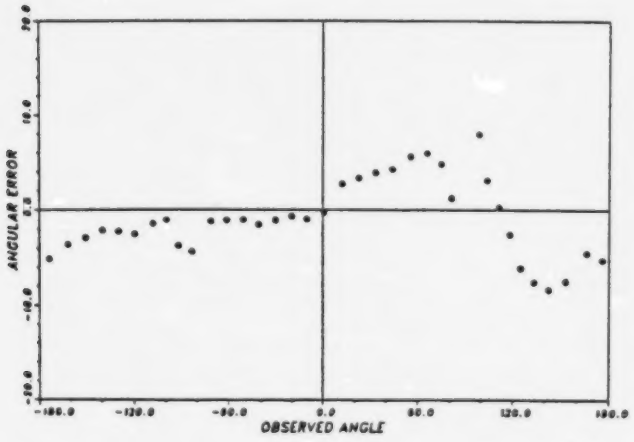

LEVEL

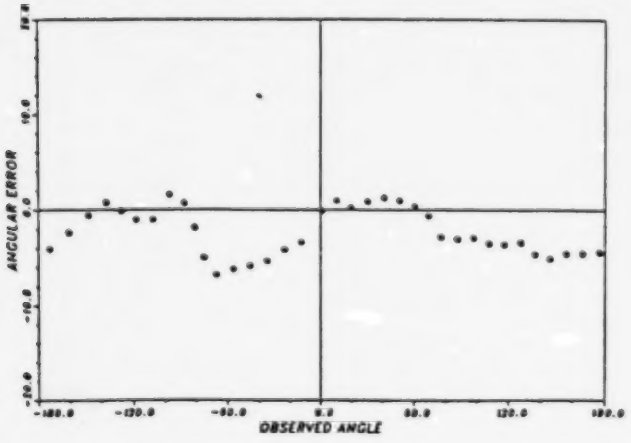

20 DEGREES
TO STARBOARD

Figure 11. DAWSON WIND ANGLES - ROLLED ORIENTATIONS
- REGULAR ANEMOMETER

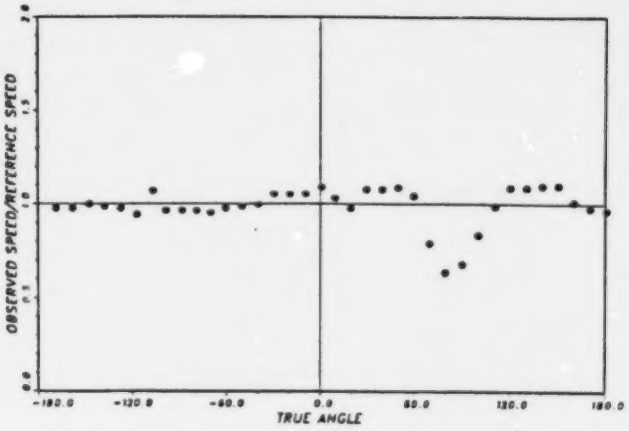

20 DEGREES
TO PORT

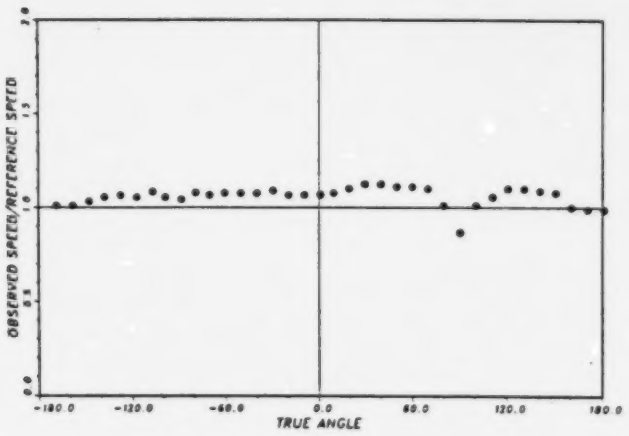

LEVEL

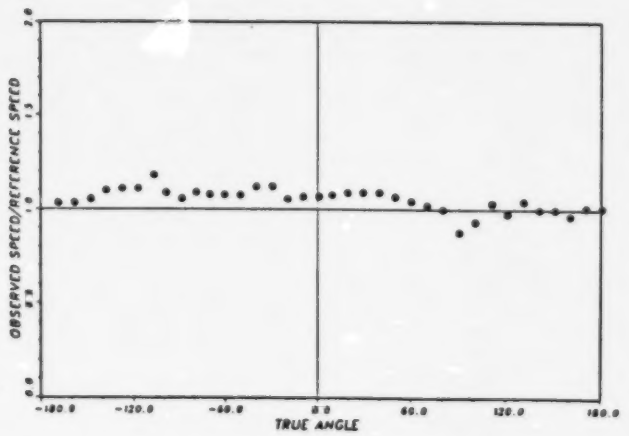

20 DEGREES
TO STARBOARD

Figure 12. DAWSON WIND SPEEDS - ROLLED ORIENTATIONS
- REGULAR ANEMOMETER

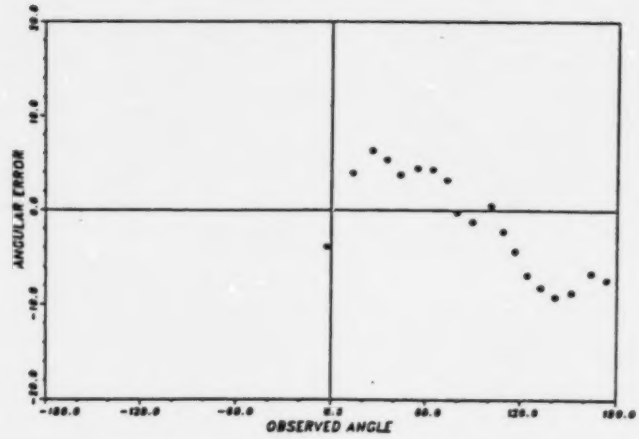

BOW UP
5 DEGREES

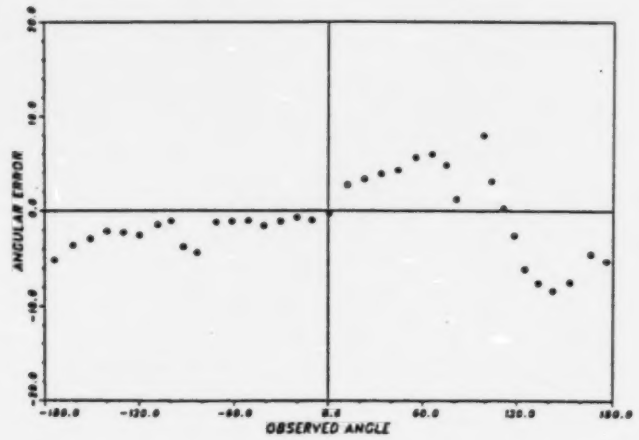

LEVEL

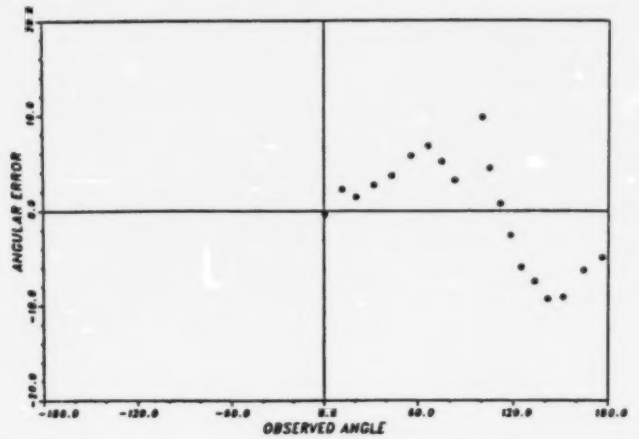

BOW DOWN
5 DEGREES

Figure 13. DAWSON WIND ANGLES - PITCHED ORIENTATIONS
- REGULAR ANEMOMETER

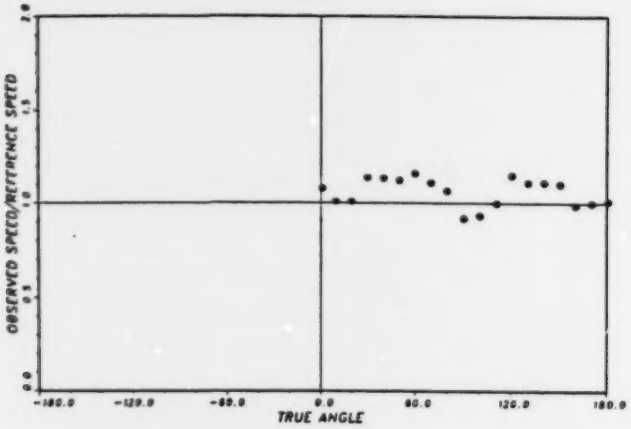

BOW UP
5 DEGREES

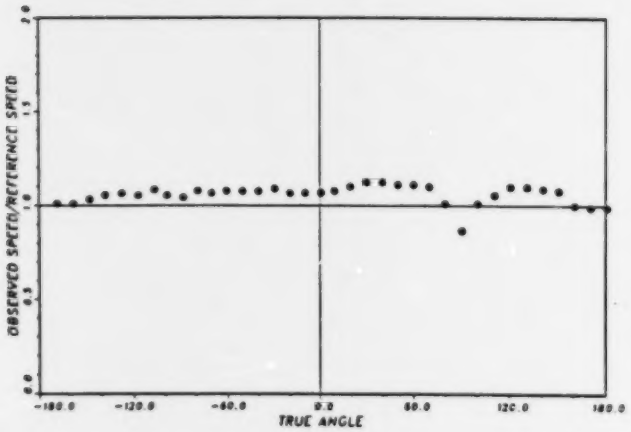

LEVEL

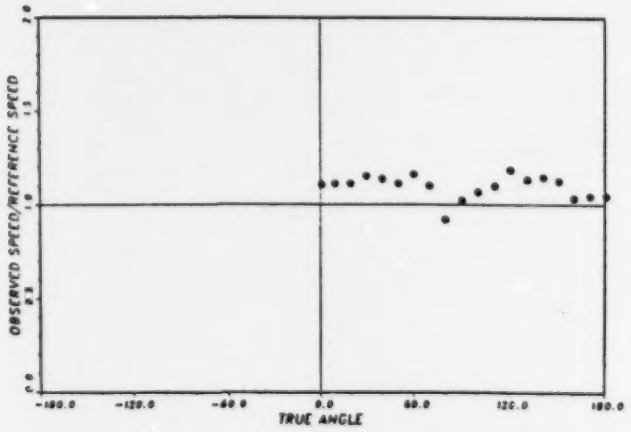

BOW DOWN
5 DEGREES

Figure 14. DAWSON WIND SPEEDS - PITCHED ORIENTATIONS
- REGULAR ANEMOMETER

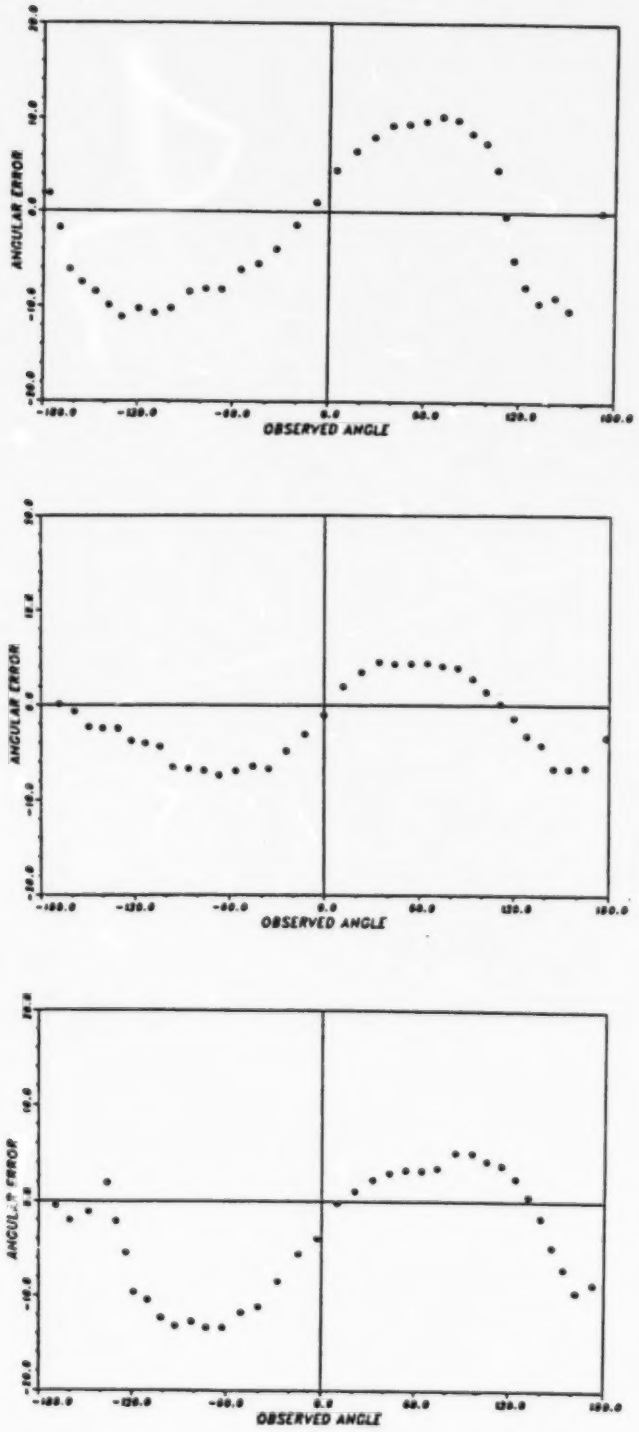

Figure 15. DAWSON WIND ANGLES - ROLLED ORIENTATIONS
- BOW ANEMOMETER

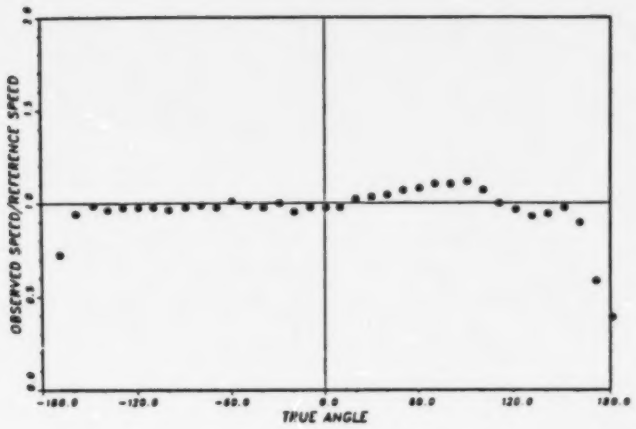

20 DEGREES
TO PORT

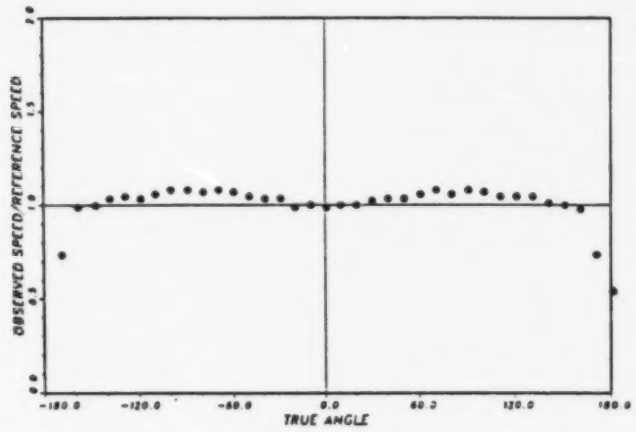

LEVEL

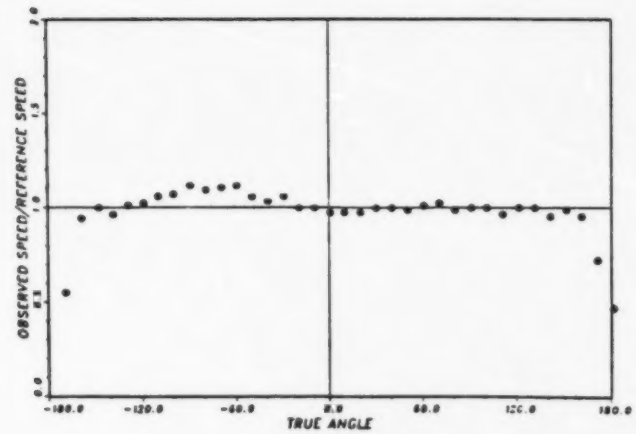

20 DEGREES
TO STARBOARD

Figure 16. DAWSON WIND SPEEDS - ROLLED ORIENTATIONS
- BOW ANEMOMETER

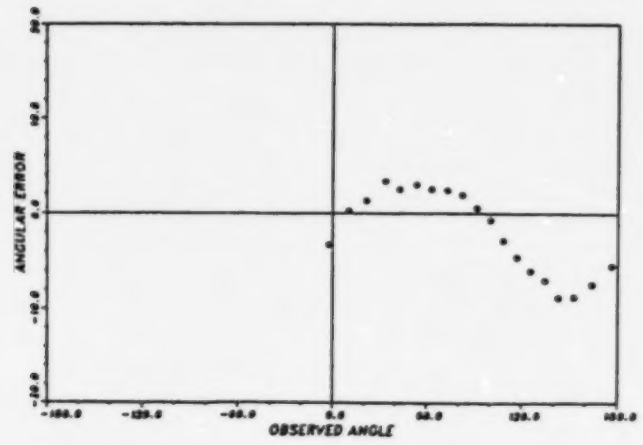

BOW UP
5 DEGREES

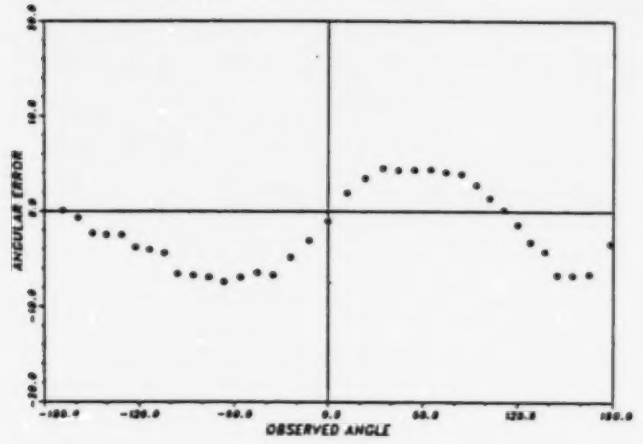

LEVEL

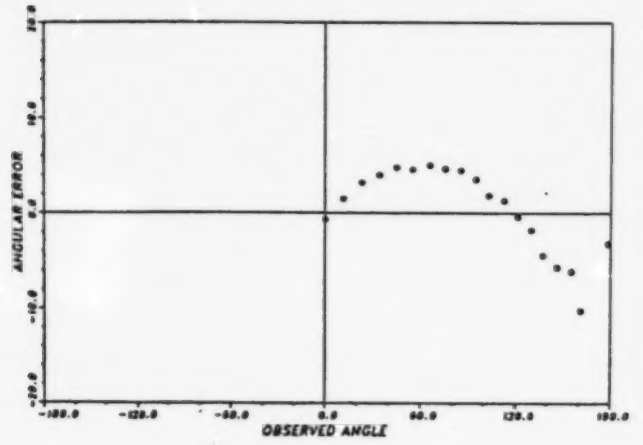

BOW DOWN
5 DEGREES

Figure 17. DAWSON WIND ANGLES - PITCHED ORIENTATIONS
- BOW ANEMOMETER

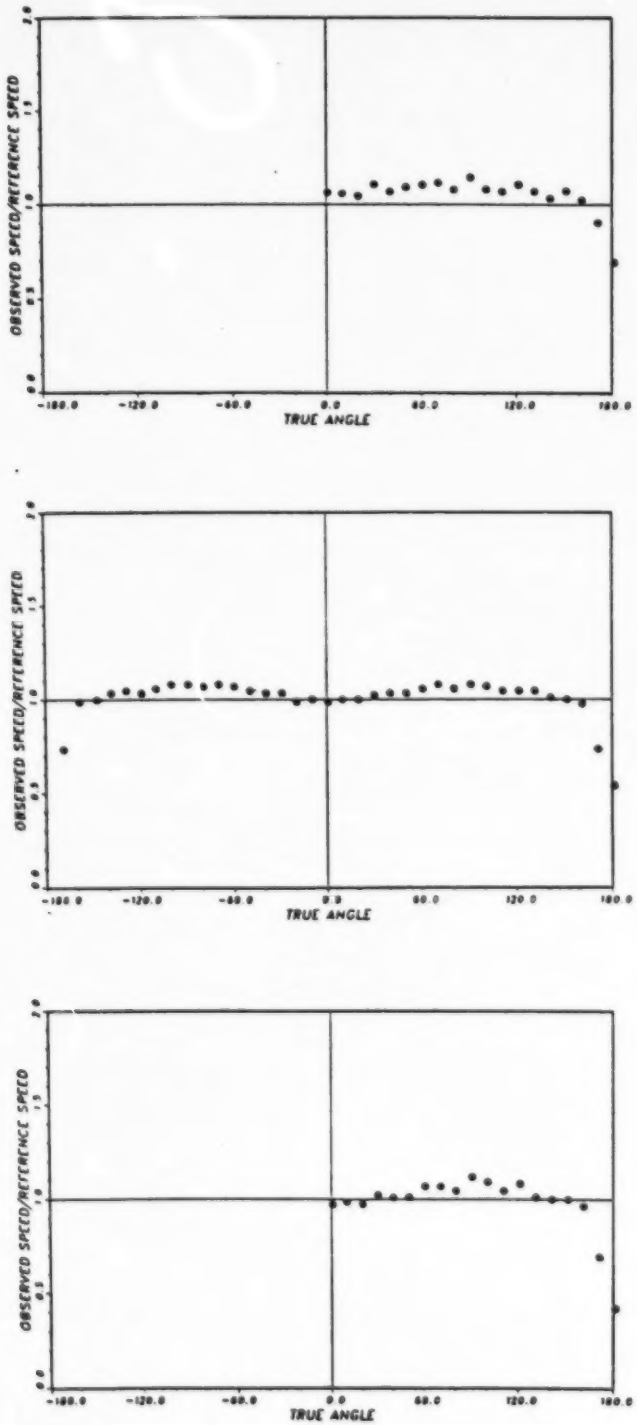

Figure 18. DAWSON WIND SPEEDS - PITCHED ORIENTATIONS
- BOW ANEMOMETER

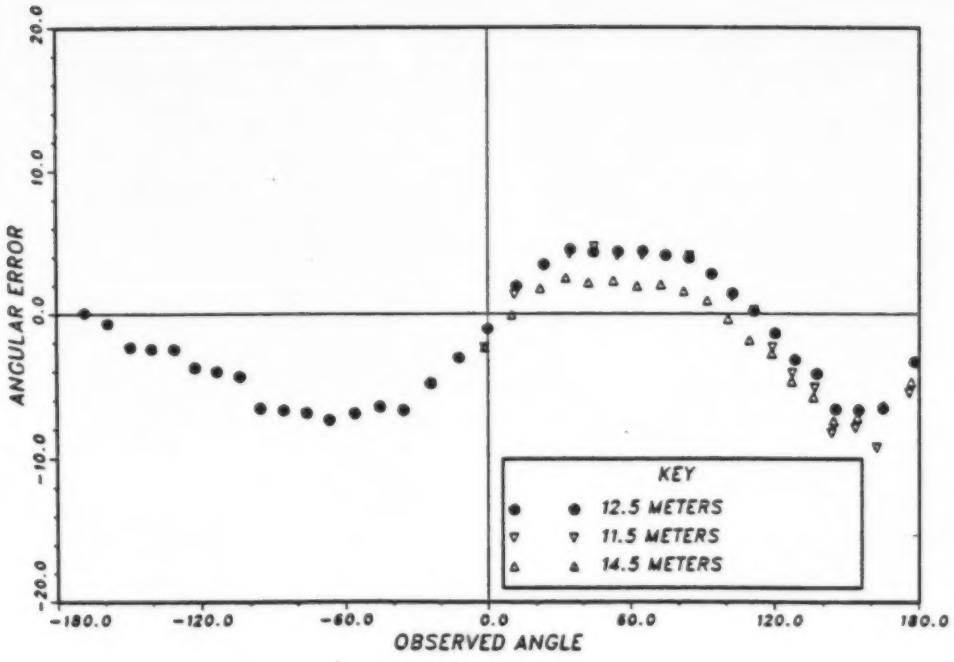

Figure 19. DAWSON WIND ANGLES - EFFECTS OF HEIGHT
- BOW ANEMOMETER

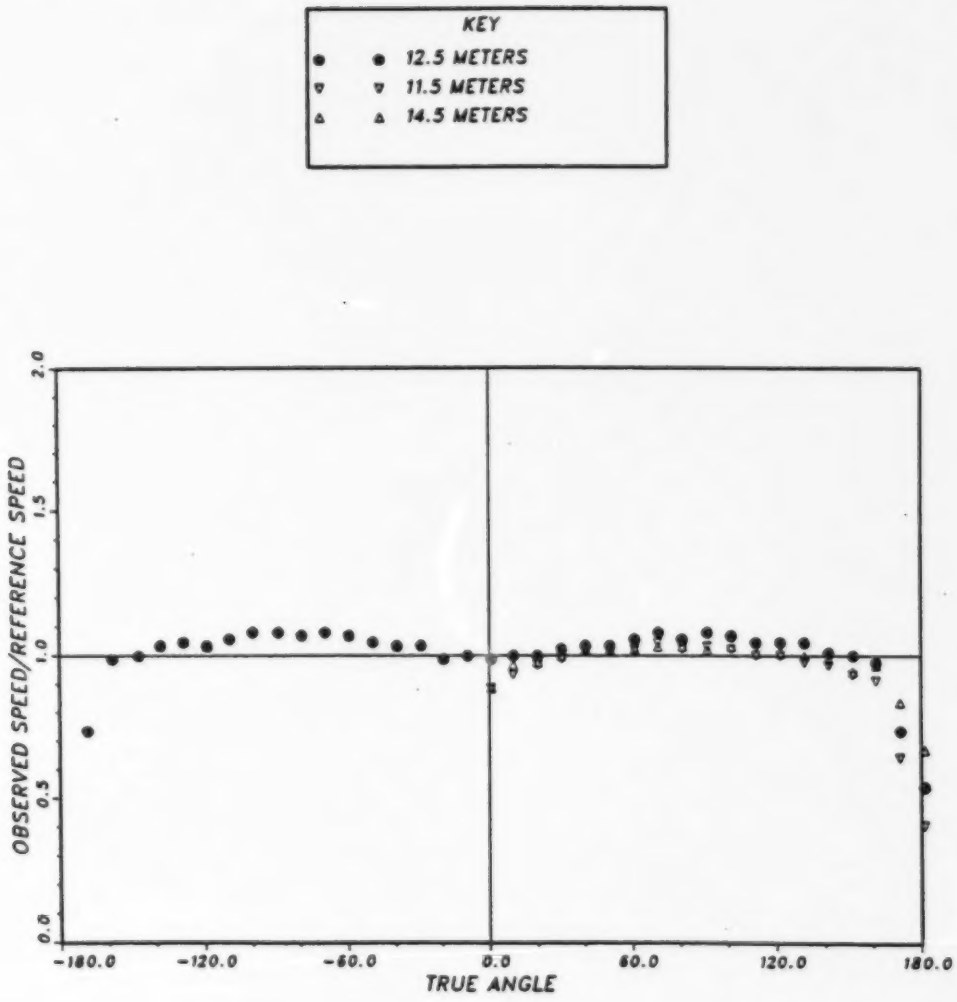

Figure 20. DAWSON WIND SPEEDS - EFFECTS OF HEIGHT
- BOW ANEMOMETER